CENTER FOR
MACHINE PERCEPTION

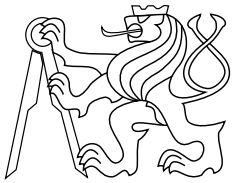

CZECH TECHNICAL
UNIVERSITY IN PRAGUE

Ph.D. Thesis Proposal

ISSN 1213-2365

Physics-Based Models for Robotic Soft Fabric Manipulation

Ph.D. Thesis Proposal

Vladimír Petrík

vladimir.petrik@fel.cvut.cz

CTU–CMP–2016–08

August 22, 2016

Supervisor: Prof. Ing. Václav Hlaváč, CSc.

This work was supported by the Technology Agency of the Czech Republic under Project TE01020197 Center Applied Cybernetics, the Grant Agency of the Czech Technical University in Prague, grant No. SGS15/203/OHK 3/3T/13.

Research Reports of CMP, Czech Technical University in Prague, No. 8, 2016

Published by

Center for Machine Perception, Department of Cybernetics
Faculty of Electrical Engineering, Czech Technical University
Technická 2, 166 27 Prague 6, Czech Republic
fax +420 2 2435 7385, phone +420 2 2435 7637, www: http://cmp.felk.cvut.cz

Abstract

Robotic manipulation of soft materials remains a challenging task due to the high degree of freedom involved. One of the studied manipulation tasks is to fold the soft fabric, e.g. garment, which lies flat on the folding surface. This task is called folding. It is one part of a complex garment manipulation pipeline, which starts with a heap of garments and ends with folded garments at the end.

The folding task is usually decomposed into individual folds according to a predefined model. A single fold is then planned and performed by a robot. Performing the single fold accurately is essential to obtain accurately folded garment at the end. Existing approaches assume the garment is infinitely flexible or rely on a comprehensive simulation. The goal of this Ph.D. thesis proposal is to provide an overview of the soft fabric manipulation pipeline with the emphasis given to the folding task. We have identified the gap in the related state of the art, which provides the opportunity for our novel contribution.

We have addressed the folding task in our previous work. Our method has been based on physics-based modeling. We also summarized our past contributions in this text. The physics used for the model together with the state-of-the-art soft fabric modeling techniques are part of our analysis too. We concluded the proposal with describing the openings in the state of the art and with the plan of future work towards the Ph.D. thesis.

Contents

1 Introduction

1.1 Robotic Soft Materials Manipulation

The automatized manipulation of soft materials has been studied intensively in the past. The manipulation of such materials is complicated because the object deforms during the manipulation. The prediction of this deformation is essential for planning the manipulation task coherently. The examples could be manipulation of a soft metallic wire, metal, kevlar or rubber sheet, fabric, or as in our study, garment.

The case explored in this Ph.D. thesis proposal is a robotic manipulation of a garment. The earliest study in robotic garment manipulation pipeline was presented by Kyoko Hamajima and Masayoshi Kakikura in 2000 [1]. The complete garment manipulation pipeline selects a piece of garment from a given heap at the beginning. The garment is then folded by a series of manipulation tasks. Many researchers addressed the individual tasks of the manipulation pipeline. We will review the individual tasks in the following sections.

One of the manipulation tasks is performing a single fold on a flat garment. This requires to grasp the garment on one side and to follow the folding trajectory. The folding trajectory depends on the material properties, in general. If properties are not considered in the trajectory design, the folding is inaccurate. The examples of inaccurate folding are shown in Fig. 1, where either the garment slips on the table or additional wrinkles form. Both situations are unfavorable in the folding. They could be avoided if the adaptive folding trajectory is used.

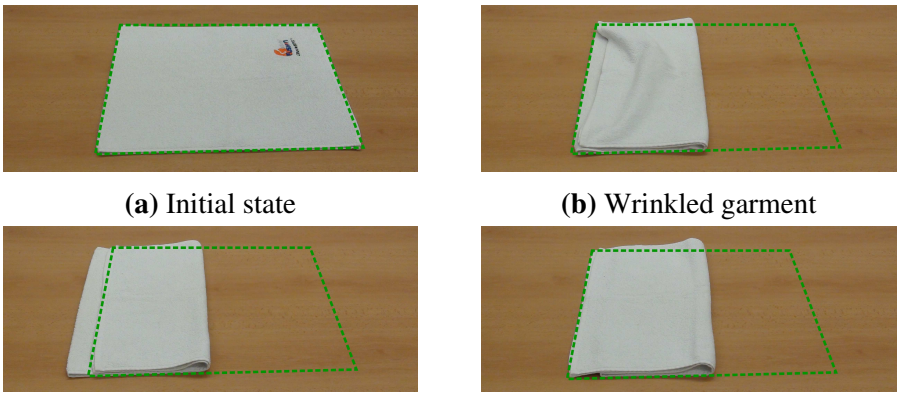

(a) Initial state **(b)** Wrinkled garment

(c) Push slippage **(d)** Pull slipage

Fig. 1. Inaccurate fold results for a towel folding. The folding starts from an initial state. A robot grasps the soft fabric on one edge only. Three different results of the folding are shown. They depend on the followed folding trajectory. Either the additional wrinkles are formed or garment slips during folding. Two slips are distinguishable deppending on whether a robot pushes or pulls the garment.

1.2 Motivation

Our previous work was motivated by the requirements of the FP7 project CloPeMa - Clothes Perception and Manipulation [2]. In the project, a unique robotic testbed was created allowing accurate manipulation with soft materials. The testbed consists of a dual-arm robot mounted on the turntable. The testbed contains various sensors allowing to measure 3D point clouds, forces/moments, or the fabric structure using photometric stereo. The accuracy of the testbed was achieved by the calibration, which was described in the technical reports [3, 4]. The verification of the calibration was provided in the technical report [5]. With the accurate robotic testbed, we were able to fold the garment on the table. However, we observed the garment is not folded accurately. The inaccuracy was caused by the folding trajectory itself since the robot was calibrated to follow the folding trajectory accurately. The garment perception and its folding using a dual-arm robot were described in conference paper [6]. The author of this Ph.D. proposal contributed to these works (i.e. [3, 4, 5, 6]). The CloPeMa testbed was used in many other experiments as will be shown in Section 2.

1.3 Problem Formulation

The aim of our work is to develop an algorithm for folding trajectory design taking the material properties into account. The designed folding trajectory should fold the garment accurately on a regular table. The physics-based garment model will be used when designing the folding trajectory. Such a garment model will be parametrized by several material properties. These properties have to be estimated if the method should work properly. The estimation of the properties in the course of folding should be addressed by our algorithm as well.

The task we are interested in is a garment folding. However, the developed techniques and models should be general for other thin elastic materials too. We would like to use the results of our research in a starting project RadioRoSo [7]. The project extends the CloPeMa project and aims to manipulate with a radioactive soft materials.

1.4 Notation

Different works used different terms to describe the same quantity in the literature. To make this thesis proposal consistent, we have used unified notation and have changed the original terms found in the literature. The most significant/confusing terms are described here.

We deal with the *garment* manipulation. The examples of the garment are a towel, shirt, t-shirt, pants, etc. The garment is often called cloth in literature.

We used the word garment to refer to the cloth in the state-of-the-art methods. The garment is made from *fabric*. We used word fabric to refer to the material from which the garment is created. Performing measurement on the fabric usually refers to a small rectangular fabric sample. The fabric is created by *weaving* or *knitting* of the individual *yarns*.

When a robot performs folding, it follows the *folding trajectory*. The trajectory is a sequence of poses of all robots grippers together with a timestamp for each pose. The gripper pose consists of the position and the orientation of the gripper. The trajectory itself defines the gripper poses in time. The time information is often omitted in the folding design because the effect of dynamics is neglected. In such a case, we used the term: *folding path*. The folding path is a sequence of gripper poses without the time information.

The Ph.D. thesis proposal is divided as follows: The robotic garment manipulation pipeline is described in Section 2.1. It is followed by state-of-the-art methods for folding trajectory design described in Section 2.2. In addition to our previous work, two other folding trajectories appeared in the literature. The first is purely geometrical and does not depend on the material properties. The second utilizes a simulated environment to predict the garment deformation for different folding trajectories. The garment model, which can be used for simulation, is not unique. Different modeling techniques for garment simulation are described in Section 2.3. In our previous work, we have addressed the folding trajectory design too. Our contributions are highlighted in Section 3. Section 4 suggests topics for ongoing research, which will lead to Ph.D. thesis.

2 State of the Art

The literature overview in this section is divided into the three main sections. First, the conventional garment manipulation pipeline is described in Section 2.1. The pipeline consists of several actions, each manipulating the garment from the start to the desired state. We are mostly interested in actions generating the folding path. This topic is studied in Section 2.2, in detail. Existing approaches for the folding path generation are shown together with their drawbacks, which form a motivation of our study. Section 2.3 summarizes several methods for soft material simulation, which we would like to use for the planning of the folding path.

2.1 Garment Manipulation Pipeline

The ultimate goal of a robotic garment manipulation pipeline is to provide folded garments stacked in one place. At the beginning of the pipeline, the garments are mixed in a heap. A single garment is isolated by a robot and manipulated until folded. The first complete pipeline was presented in [8], where a PR2 robot was used to fold a towel. Their towel specialized approach could be generalized into the following steps:

- garment picking from a heap,
- garment type classification,
- unfolding,
- flattening or ironing,
- folding,
- stacking.

More recent work [9] used this pipeline to fold wider range of garment types including a t-shirt, pants, and sweater. The folding pipeline is visualized in Fig. 2.

2.1.1 Picking

Basically, the picking is a pre-processing step assuring a single garment is held by a robot gripper. The isolating of the single garment from the heap is required followed by the grasp point detection. One of many methods for robotic picking was reported in [1]. The isolating of the single garment was performed based on the recursive color segmentation. It was assumed that garments are distinguishable by color only and that single garment has a unique color. The grasp point was selected to be in the middle of the largest obtained color region. Specially designed gripper was then used to grasp the garment.

Other methods used the combination of color and depth measurements to find a grasp point. For example in work [10], the highly wrinkled point was selected.

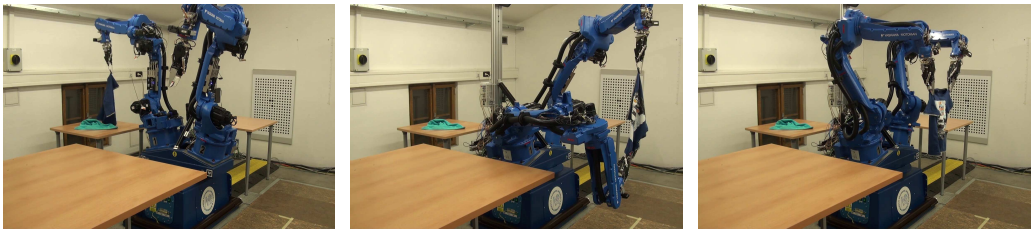

(a) Picking **(b)** Unfolding **(c)** Unfolded

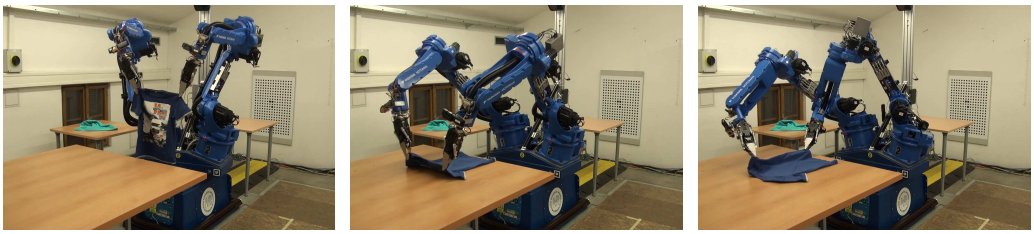

(d) Preparation for laying **(e)** Laying on table **(f)** Folding

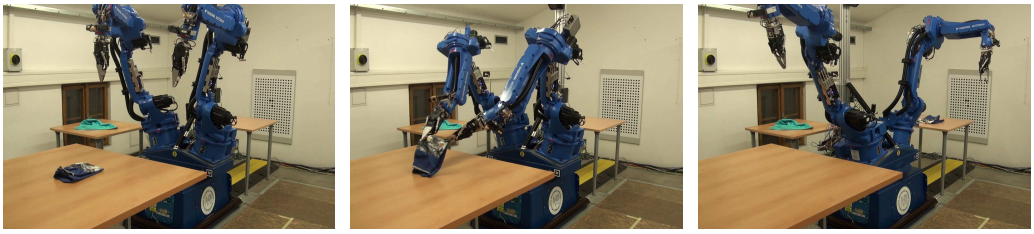

(g) Folded **(h)** Stacking **(i)** Stacked

Fig. 2. The garment manipulation pipeline performed by a CloPeMa robot. The flattening step is omitted in visualization. The classification is done in the course of unfolding.

The authors of towel folding pipeline [8] used a discontinuity of depth measurement to estimate a curvature for a grasp point selection. Several modifications exist selecting the grasp points based on height, color, shape, etc. The benchmark for the various grasping strategies was provided in [11].

2.1.2 Classification

The picking itself requires no information about the type of the garment. However, the type is expected to be known to perform unfolding and folding. Further, the current pose of the garment needs to be estimated as well.

The pose recognition of the single garment type (pullover) was studied in [12]. The authors utilized mass-spring physics-based simulation to compute the free hanging garment shapes for different grasp points. The simulated shape was matched to a real image. The best match was used as a garment pose estimation. The method was extended in [13] to simulate several garment types and to

provide the pose together with the type of the garment. The next extension [14] used reconstructed point cloud and animation software *Autodesk Maya* to evaluate the best match for the garment type and pose. This method was used in combination with a robot in [15, 16]. Both works used an active manipulation - the garment was actively manipulated to gain missing information for the underlying simulated model.

Another work [17] used depth measurement as well to obtain the pose and type of the garment. The real robotic experiments were used to train an SVM classifier in a training phase. The classifier was then used to categorize acquired depth measurement.

To simplify the classification task, an active manipulation was used in [18] to bring the garment into its limited shapes prior to classification. The limited shapes are characteristic poses of the garment obtained by predefined manipulation steps. After a few manipulation steps, there is a finite number of possible garment poses for the given garment type. Such an approach simplifies the final classification but relays on bringing the garment into its limited shape.

The more recent classification method [19] used the active manipulation too, but the method is iterative. The robot updates the garment pose until the confidence is sufficiently high. The method was integrated into the pickup stage and was able to categorize highly wrinkled garments. Since the active manipulation is often involved in recognition, many researchers perform the classification in the course of unfolding as will be shown in the next section.

2.1.3 Unfolding

The unfolding starts with the garment held by a single arm. The first approach for unfolding [20] used a dual-arm robot and relayed on a unique garment color and on a simple background in order to simplify a vision segmentation task. The segmented result guides the robot to re-grasps the garment until both grippers held the garment corners. The method was able to unfold several garment types without knowing the type in advance. In the paper, the categorization of the garment was performed based on the image matching after the unfolding. The similar approach was used for towel unfolding in [8], where the corners were detected for the towel unfolding. The goal was to hold two corners of the same edge and then untwist the gripper if necessary.

The method described in [21] was able to unfold various garment types by re-grasping of the lowest point of the garment. The type of the garment was recognized during the re-grasping. After the type had been recognized, the garment was laid on the table and unfolded by series of manipulation steps. Improvement of this work was provided in [22], where the garment was unfolded without laying it on the table. Furthermore, the performance of the unfolding was improved by

decreasing the number of required grasping operations. Both approaches [21, 22] used a probabilistic framework to represent the garment pose and type.

Another method for unfolding [9] represents the garment in the animation software *Autodesk Maya*. The iterative re-grasping method was used to estimate the garment type/pose and to bring the garment into the desired configuration afterward.

Automatic action selection for the unfolding of the towel was presented in [23]. Authors used two possible actions for unfolding: a garment lifting and a pinch and slide motion. Robot selects the action automatically based on a partially observed Markov decision process.

The most recent method for the unfolding was presented in [24]. The garment is brought in an approximately planar configuration, where the garment is simply folded. This configuration is achieved by re-grasping the garment in the air. After it is approximately planar, the garment is laid on the table. The template matching technique is utilized to detect the simply folded garment. Robot lifts the garment afterward to bring it to its unfolded configuration.

2.1.4 Flattening

After the unfolding stage, either the unfolded garment is held by both grippers in the known configuration, or it lays on the table already. If a former situation occurs, the garment is laid on the table by pulling it over a table edge. Now, the garment lays on the table freely, and robot grippers are empty. However, small wrinkles could be presented on the garment. They need to be removed before folding to obtain the accurate folding result. This process is called flattening.

Preliminary work on flattening was presented in [25]. A single arm robot was used to pull the garment at various places on the outer boundary. The direction was computed to pull from the centroid of the garment. It removes the major wrinkles and authors considered a situation in which part of the garment remains unfolded. The depth sensor was used to localize these unfolded parts, which were removed by a robotic arm afterward.

The wrinkles detection in a simulation was presented in [26]. The work describes the detection of the largest wrinkle together with an estimation of the pulling force and its direction. The method operates on the 3D point cloud obtained from the simulation. The method itself is iterative - repeated until the garment is flat to the certain threshold. The same approach was used in a real robotic testbed in [27]. The largest wrinkle was detected on an accurate depth measurement obtained from a stereo reconstruction. Moreover, the method was extended to a dual arm robot, reducing the number of required iterations (Fig. 3).

Described methods perform flattening using the pulling operation only. The more advanced method presented in [28] uses an iron to remove the wrinkles from

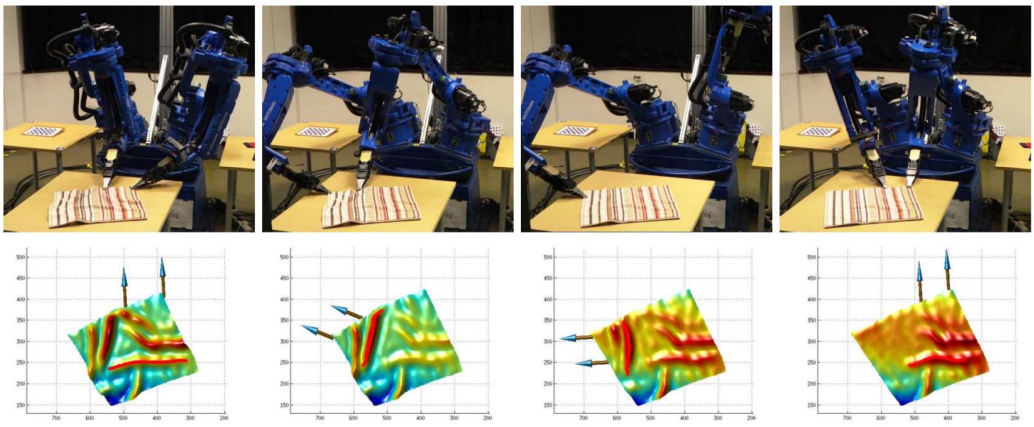

Fig. 3. Flattening of a towel performed by a CloPeMa robot. A real flattening (top) together with the reconstructed model and detected wrinkles (bottom) is shown. The arrows in the model suggest the direction of pulling for removing the largest wrinkle. In a third image, a single arm was used because following a dual arm path was not feasible. Images are from [27].

roughly flattened garment. Described method estimates regions which need to be pulled in prior of folding and other regions, which could be ironed directly. The ironing is then performed on the whole surface providing the flattened garment at the end.

2.1.5 Folding

A folding starts with a flattened garment, which lays freely on the table. The folding of the garments with dual arm robot was described in [29]. The method detects the pose of the garment on the table using the approach described in [30]. With a known pose and garment type, the folding is decomposed into individual folds. Each fold is represented by a folding line - the oriented line dividing the garment into a fixed and moving part (Fig. 4). While folding, the robot moves the moving part on the top of the fixed part. It is repeated until all folds are performed. There exist several approaches how to move the moving part on the top of the fixed part, and they will be described in Section 2.2.

The improvements to the folding pipeline were proposed in [6]. Authors improved the segmentation algorithm allowing to fold the garment on a regular table with non-uniform color. Furthermore, the detection of the garment was performed after each fold. It improves the robustness since the garment can be moved on the folding surface during the robotic manipulation.

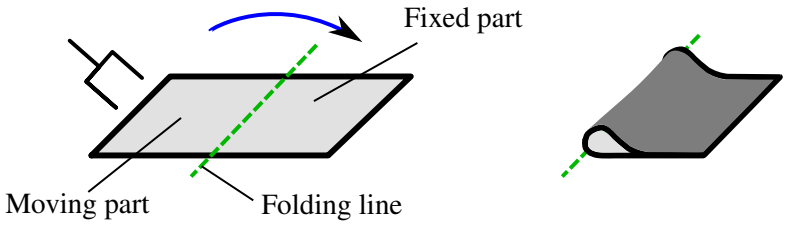

Fig. 4. The folding visualization for the simplest scenario, where the folding line (green, dashed) divides the garment into two equally sized parts. The one side of the sheet is grasped, and the folding trajectory is followed to move the moving part on the top of the fixed part.

2.1.6 Stacking

The stacking is a post-processing step. It is used to free the folding table and thus to prepare the testbed for the folding of the next garment. In our previous unpublished work, we have stacked the garments on a separate table. Since the folding result is a rectangular shape usually, the stack is detected on the stacking table using oriented bounding box fitting. Then robot moves the folded garment on the top of the stack.

2.2 Performing a Robotic Fold

As stated above, the folding composes of several folds. In a single fold, the robot moves the moving part of the garment on the top of the fixed part. The individual parts are determined by the folding line. The example of the single fold is shown in Fig. 4. In this particular example, the folding line is aligned with the towel edges, and it is in the middle of the garment. It describes the simplest folding scenario, in which the moving and fixed parts have the equal size.

Performing the fold by a robot requires generating a trajectory for individual grippers of the robot. However, the existing approaches generate the folding path only. The folding path is followed slowly so that the garment dynamics does not influence folding. Several approaches for the folding path generation exists - each making different assumptions about the garment. These assumptions limit the method to particular garment material and if the assumptions are not met it will result in an inaccurate or incorrect fold.

2.2.1 Gravity-Based Folding

The first method generating the folding path for robotic folding was shown in [31]. It is called a gravity based fold or a *g-fold*. The paper describes a geometric model of the garment, which is based on the following assumptions:

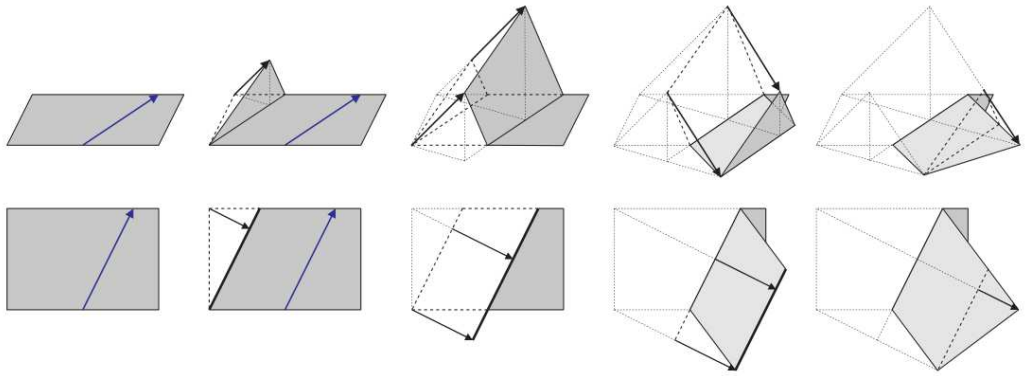

Fig. 5. The linear gravity based folding visualization for a towel. One fold performed by two grippers is shown. Blue arrow represents the oriented folding line. Images are from [31].

- The garment is non-stretchable with zero thickness.
- The garment is subjected to gravity.
- The garment has no dynamics.
- The garment has infinite friction with the surface on which it lies and with itself.
- The garment has infinite flexibility.

The first assumption is a good approximation since the most of the garments are not significantly stretchable and are thin. The second assumption is valid during the folding. The garment dynamics can be neglected if the garment is moving relatively slowly. In such a case, the effect of the dynamics on the pose of the garment is small. The slow garment motion could be achieved by a slow robot motion.

The last two assumptions are not satisfied in a real robotic folding. The friction between the garment and the folding surface (regular table) is finite and often not very high. With finite friction, the garment has a tendency to slip on the table when folding with the g-fold path. To overcome this problem, authors used a specially designed table, which had a large friction coefficient.

The infinite flexibility assumption is also unrealistic. The typical garments resist to a bending deformation. For example, the bending resistance of the denim fabric is larger than bending resistance of the satin fabric. When the gravity based folding is used, the folding of the satin material is thus more accurate than folding of the denim material.

If these assumptions are satisfied, the folding path consists of a set of line segments as shown in Fig. 5. The simplicity of the g-fold approach lies in a fact that no physical simulation is required to obtain the path. The method is purely geometrical. However, ignoring of the material properties might result in an inac-

curate folding. Nevertheless, the methods showed to be a good approximation for a wide range of garment materials if a specially designed table is used and if the folding accuracy requirements are not high. Since there will be another gravity based folding path in the Section 3, we will refer to this path as *linear folding path*, hereinafter.

2.2.2 Predictive Simulation and Trajectory Optimization

To overcome the problem of the garment slipping, the simulation was used in work [32]. Authors estimated the material parameters and then performed the folding virtually in a simulation. The folding path was then perturbed until the virtual folding was accurate enough. The path was performed by a real robot afterward.

Animation software *Autodesk Maya* was used for the simulation. The simulator utilizes a mass-spring network to simulate the garment. In the Maya, it is called '*nCloth*' simulation. The simulation consists of n particles connected by springs with a specific stiffness. The physics of such simulation is straightforward but according to [33] there are some significant drawbacks:

- The simulated garment behavior depends on the spring network structure.
- It can be difficult to tune the spring constants to get the real garment behavior.

On the other hand, the *nCloth* simulation is effective, thus often used in computer graphics or animation software. The simulation allows to set following material properties:

- stretch and compression resistance,
- bend resistance,
- bend angle dropoff,
- shear resistance,
- restitution angle and tension,
- rigidity,
- and deform resistance.

Such parameters allow simulating various effects including elasticity, hysteresis, or bending.

From all available parameters, authors of [32] observed that the shear resistance affects the simulation in the most significant way. The other parameters were fixed to its default values, and only the shear resistance was adjusted to tune the simulated model. The following steps were used for tuning:

- One extremum of the garment is manually picked and hanged under the gravity.
- The total length of hanged garment is measured and denoted by symbol L_1.

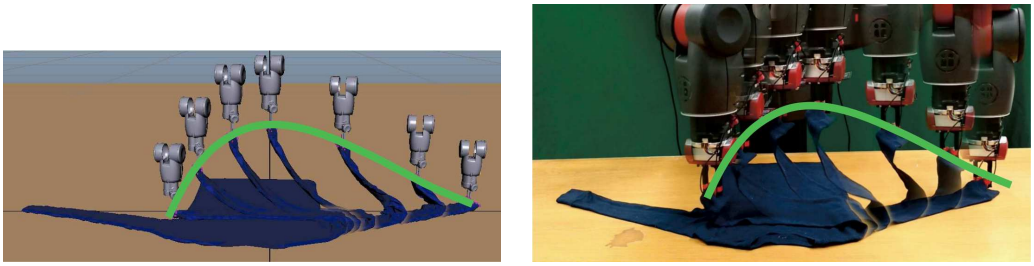

(a) Simulated folding **(b)** Real folding

Fig. 6. The predictive simulation of the folding. The figure shows a planned path performed both, in simulation and real folding. A Baxter robot was used for robotic folding. Images are from [32].

- The garment is then laid on the table slowly. The total length of laying garment L_2 is measured.
- The shear resistance fraction is computed: $shear\_frac = \frac{L_1 - L_2}{L_2}$.
- The shear resistance of the simulation is then tuned until the simulated shear resistance fraction is identical to the measured one.

Another property, which influences the folding path, is the friction between the garment and the folding surface. Authors lifted one side of the table until the freely laid garment started to slide. The inclination angle of the table was measured at that moment. The simulated friction was set such that the minimal table orientation required for the garment sliding was equal in the simulation and reality.

The parameters were measured by the authors before the folding started. The garment was then folded virtually using the path described by a Bézier curve. The virtual fold quality was evaluated by comparing the expected pose and the simulated result. The path was optimized until the simulated result was satisfactory. The folding path was then performed by a robot as shown in Fig. 6.

This approach for folding path generation was used to fold various garment materials. However, authors observed the folding of the denim material is less stable. It is caused by the fact that the shear resistance is relatively large for the denim. In our work, we use another physics-based model to generate the folding path taking the bending resistance into account. We will describe the method in Section 3.

2.3 Garment Physics-Based Simulation

The accurate simulation of the garment remains a complicated task due to the garment internal structure. The simulation can be divided into two scales [34]:

- yarn scale,

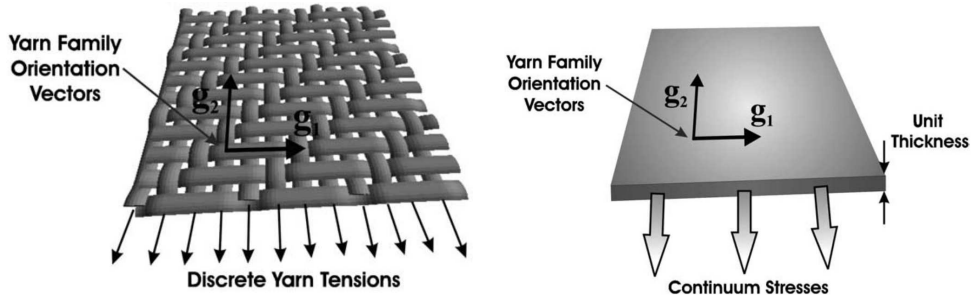

(a) Individual yarns of a fabric structure **(b)** Macro-mechanical approximation

Fig. 7. Fabric approximation as an anisotropic continuum. Vectors $\boldsymbol{g}_1$ and $\boldsymbol{g}_2$ represents '*weft*' and '*warp*' yarns directions. Images are from [35].

- and macromechanical scale.

The yarn-scale simulation studies individual fibres or yarns, of which the fabric is created. The yarn mechanical properties are considered together with an interaction between yarns. The interaction involves the contact modeling, the internal friction modeling, or the yarns connection pattern modeling.

The macromechanical scale is a result of yarn homogenization. Instead of discrete yarns, the fabric is considered to be a continuous medium. The garment simulation at the macromechanical scale is derived based on continuum mechanics, and individual yarns affect the mechanical properties of the fabric continua. Both scales are visualised in Fig. 7.

2.3.1 Yarn Models

Yarn-based simulation models the yarns of the fabric explicitly. Several models exist, each making different assumptions about the individual yarn properties. The first model was proposed in [36], where the fabric was simulated purely geometrically. The yarns were considered to be infinitely flexible and inextensible with a circular cross-section. The model was used to simulate woven fabric. Because the geometry in [36] is detailed, the simpler model was proposed in [37]. Authors model the biaxial, uniaxial, and shear deformation behaviors of fabrics based on pin-joined truss geometry. Both works [36, 37] considered plain weave fabric with persistence yarns contacts (no yarn slippage). The extension to non-plain weave fabrics was provided in work [38].

The methods showed above considered the structure and geometry of the yarns pattern only. The more advance method [39] was shown for plain weave fabric (*Kevlar*), where the inter-yarn friction was modelled. The individual yarns were modeled as cylindrical rods.

In series of papers [40, 41, 42], another yarn-scale simulation was proposed.

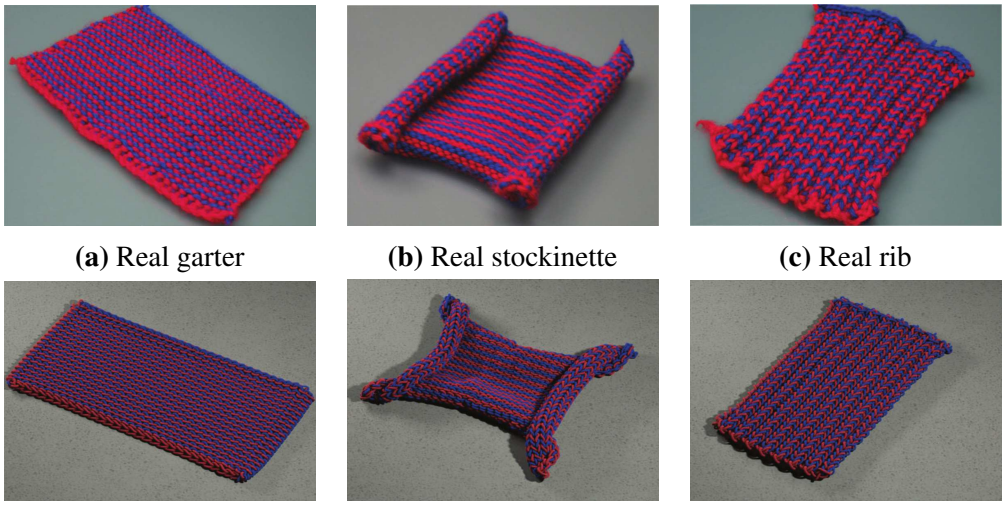

(a) Real garter **(b)** Real stockinette **(c)** Real rib

(d) Simulated garter **(e)** Simulated stockinette **(f)** Simulated rib

Fig. 8. Visual comparison of the real (top) and simulated (bottom) knitted garments. A garter, stockinette, and rib patterns are compared. Images are from [42].

Authors model the knitted garment behavior based on the individual yarns modeled as inextensible rods. The yarn-yarn contact was considered together with velocity filter for the friction approximation. The visual comparison of modelled and real knitted fabrics was conducted for various knitting patterns showing visually good match (Fig. 8).

The more efficient method for yarn-scale simulation was shown in [43]. Authors implemented yarn-yarn contact, which is able to represent inter-yarn sliding efficiently. Simple force model was used to simulate friction and shear effects. The GPU parallel time integration was proposed to speed-up the simulation. The fabric nonlinear behavior was simulated, but the results were not compared with real fabric yet.

The yarn based simulation is physically accurate, but it is computationally expensive. Typical fabrics consist of many yarns per centimeter, which limits the simulation to small fabric samples only. To make it tractable, the simulation of the friction and contacts is often approximated, which affect the accuracy. Furthermore, estimation of the parameters for individual yarns is a nontrivial task as well. These disadvantages lead to the lower scale simulation known as a macromechanic-based continuum simulation.

2.3.2 Macromechanic Models

The macromechanic model of fabric is a result of homogenization of the individual yarns. The fabric is modeled as a continuous medium with mechanical

properties. Individual yarns and their interaction affect these properties, often resulting in a nonlinear relationship between macromechanical parameters. For woven fabric, the undeformed yarns pattern is orthogonal and the orientations of the yarns are called '*weft*' and '*warp*' (Fig. 7).

The macromechanical properties of the fabric could be derived from yarns properties as shown in [35]. The yarn was assumed to be linearly elastic with linear bending resistance. Simplistic model of the yarns interaction was used where the interactions were captured by a non-linear 'interference spring'. Authors claimed, the approximation is sufficient since only a planar analysis were conducted. No yarn slippage was considered in the work. Based on these assumptions, the finite element model was derived. The developed model required 24 constitutive properties to be defined. Many experiments were performed to shown the validity of the model for the plain weave planar fabric modeling. The *Kevlar S706* material was used in the experiments. The model was then extended to account for yarn slippage in [44] and in [45]. All these methods were derived considering the yarns properties and their interactions. It leads to complicated models, which consist of 24 parameters at least. To reduce the number of required parameters, several researchers approximated the fabric continua more significantly and used shell elements for the garment behaviour prediction.

In work [46], the nonlinear shell finite element method was used for a drape prediction of fabric. The method combines membrane elements with plate bending elements. Authors compared an isotropic and orthotropic linear elasticity and reported that the orthotropic is more appropriate for fabric modeling. Another orthotropic linear elasticity model was proposed in series of works [47, 48]. Authors used degenerated shell elements, where a 3D solid element is degenerated into the shell surface element. A linear relation between bending stiffness and Young's moduli was assumed. Experiments were performed, and obtained results indicated that the linear elastic model is an acceptable assumption for the fabric drape. However, the linear elasticity assumption is acceptable for a plane strain only. The linear bending stiffness/Young's moduli relation derived from continuum mechanics is often invalid for fabrics due to its internal structure. It was studied in [49], where the bending stiffness was assumed to be independent of Young's moduli.

Another shell formulation for fabric simulation was proposed in [50]. Authors used geometrically exact shell theory and isotropic linear elasticity assumption. Nonlinear moment/curvature relationship with hysteresis was used in the simulation. Authors conducted experiments for manually folded fabrics. The resulting shape was compared with the prediction, and good agreement was found.

Only few of many existing approaches for fabric macromechanical simulation were mentioned in this section. The approaches differ in assumed model limitations. For example, several researchers studied non-orthotropic elasticity, hyper-

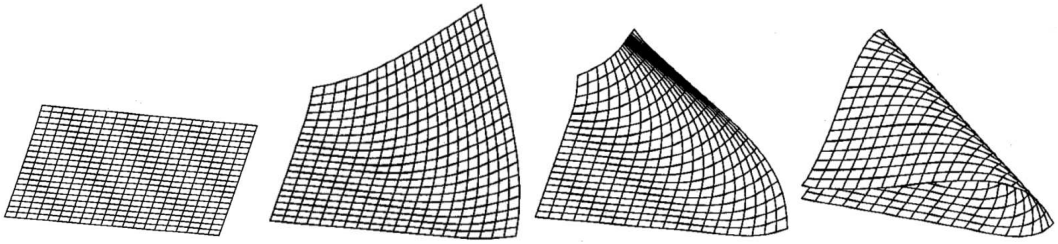

Fig. 9. Diagonal folding of the rectangular garment. The folded shape was achieved by following a circular folding path. Images are from [50].

elasticity, or additional plasticity effects. A comprehensive reviews were done in works [51, 52, 34]. These reviews compared different constitutive relations for 2D materials used for fabrics. To simulate garment in 3D, the kinematic description has to be provided as well. Different kinematics are described by different shell models as will be shown in the next section.

2.3.3 Shell Modeling

Thick and thin shells are modeled differently in the classical shell theory [53]. Thick shells are described by *Reissner-Mindlin* theory, where transverse shear deformations are taken into account. For thin shells, the *Kirchhoff-Love* theory is used neglecting the transverse shear deformations. Since garments are of complex shapes usually, the finite element methods (FEM) are applied to simulate the shell.

According to [53], using the *Reissner-Mindlin* theory for thin shells in FEM results in a phenomenon called locking. If the locking occurs, the predicted behaviour is stiffer far greater than would be expected. It makes the theory unusable for garment folding prediction as the garments are typically thin. *Kirchoff-Love* theory does not show the locking phenomena, but it is more difficult to derive its FE formulation. The circumstance lies in a fact that basis function for FEM requires to be C^1 continuous for *Kirchoff-Love* theory.

Kirchoff-Love theory is based on the following assumptions:

- The thickness of the shell is assumed constant and small with the comparison to its overall size.
- Vectors normal to the middle surface remain straight and un-stretched after deformation.

These assumptions neglect the shear deformation. The derivation of *Kirchoff-Love* shell theory was described in a series of works [54, 55, 56]. This theory was utilised for rectangular fabric folding prediction in [50]. The folding evolution is shown in Fig. 9.

The simulation of non-rectangular fabric according to *Kirchoff-Love* shell theory was achieved in [57]. Author ensures the C^1 continuity by using a subdivision-

surface concept for shell modeling. The method was then used to simulate garment with wrinkles in [58].

Another method for *Kirchoff-Love* theory FEM was proposed in [59]. Authors utilise a discontinuous *Galerkin* finite element method weakly assuring the C^1 continuity. The formulation was derived for nonlinear elastic shells later in work [60]. This finite element formulation was used in computer graphics to simulate detailed cutting of shells [61, 62].

Both formulations [57, 59] assume geometrically linear strain, which is not suitable for large rotational deformations. To overcome this problem, a *corotational* formulation [63] can be used. In the *corotational* formulation, the rotation of the element is extracted, and the forces are computed for an un-rotated element. Then the computed forces are rotated back to the original element orientation.

A geometrically nonlinear finite element formulation was proposed in [64]. In geometrically nonlinear formulation the *corotational* formulation is not required. The geometric exactness was achieved by using NonUniform Rational B-Splines (NURBS) as basis functions. The method was used for garment simulation in works [65, 66].

3 Our Previous Work

We have studied the folding path generation in a series of conference papers. First of all, we have proposed another gravity based folding method based on the circular path instead of linear. The circular path results from the assumption of rigid material with flexibility in the folding line only. We provided an analysis of the pushing/pulling force for both, the linear and circular path. Both paths were experimentally compared, and it was shown, that the circular trajectory is more suitable for some types of garments. In the same contribution, we have analyzed the folding feasibility, which is limited mostly by the robot kinematics. We have proposed several kinematics relaxations, and we have designed a closed-loop planning algorithm for the folding path generation. The work was presented in [67], and the reprint of the contribution is available in Appendix A.

Our next conference paper [68] describes a folding path generation based on the physics-based model. A rectangular homogeneous garment was assumed to simplify the analysis. Under these assumptions, a model of the garment was proposed. It was shown that the garment could be described by a single parameter, which is a weight to stiffness ratio. The folding path was found by finding the equilibrium of static forces. The equilibrium was described by boundary conditions and resulting boundary value problem was solved in order to find the garment state. The sequence of the garment states was used to define the folding path for the robotic folding. It was experimentally compared with the linear and circular path, and our model based path outperformed both. Reprint of the contribution is available in Appendix B.

In [69] (Appendix C), an analysis of our physics-based folding path generation was provided. Currently, a weight to stiffness ratio is estimated in advance of folding. The estimation is not precise, and inaccurate estimation leads to inaccurate fold. We have analyzed the effect of the inaccurate estimation on the resulting fold. The virtual and real experiments were conducted to verify our model of the garment. Based on the experiments, we have proposed a methodology, which from a given range selects the weight to stiffness ratio producing the best fold. The methodology selects the value on the pliable end of the range. We have shown, that only four weight to stiffness ratio values could be used to fold all typical fabrics.

4 Openings for Novelty in the Ph.D. Thesis

The main goal of the thesis is to provide methods for accurate garment folding. The requirements for accurate physics-based simulation of the garment was demonstrated in Section 3. Although our physics-based method for rectangular homogeneous garments outperformed the state-of-the-art methods, open problems and opportunities for improvement remain:

- **Non-rectangular garments.** The main drawback of our current method is the limitation to the rectangular garments. The extension to more complex shapes (e.g. a t-shirt, pants, etc.) would require the shell finite element modeling as was described in Section 2.
- **Properties estimation.** The current folding path generation algorithms require the material properties to be measured before the folding. This process is performed by an operator. However, it can be done by a robot in the future. In such a case, the folding would be fully autonomous. The more advanced methods could estimate the material properties in the course of folding to reduce the folding time.
- **Assumed bending stiffness linearity.** In our most recent work, we have observed the garment model does not predict the reality accurately in all situations. It is probably caused by the missing non-linearity (especially a hysteresis) in a curvature/bending stiffness relation. Many researchers identify that this non-linearity is caused by the garment internal structure and the friction between yarns, as shown in Section 2. The extension of our model taking this non-linearity into account would be required to provide a more complex analysis, for example, for unfolding or flattening of the garment.
- **Assumed homogeneity.** Only a few of garments are homogeneous in reality. In fact, most of the garments contain varying number of layers, seams, or pockets. The homogeneity assumption is violated. It complicates the garment simulation and the estimation of the garment properties. To resolve this issue, we would like to perform folding in a closed-loop manner. We would like to measure the garment shape during the whole folding, and to adjust the model and folding path according to the observed shapes.
- **The scope of materials.** We focused on the garment manipulation so far. However, the developed methods could be used for a wider range of materials. We would like to extend methods scope to be useful for other soft material robotic manipulation tasks.

References

[1] K. Hamajima and M. Kakikura, "Planning strategy for task of unfolding clothes," *Robotics and Autonomous Systems*, vol. 32, no. 2, pp. 145–152, 2000. 3, 6

[2] "Cloth Perception and Manipulation - CloPeMa," http://clopema.eu/, 2012–2015, 7th Framework Programme for Research and Technological Development. 4

[3] Z. Šika, P. Beneš, M. Valášek, V. Smutný, V. Petrík, and P. Krsek, "Calibration research of Robots within CloPeMa Project using RedCaM Arm," Czech Technical University in Prague," Research Report, 2013. 4

[4] P. Beneš, V. Petrík, Z. Šika, and M. Valášek, "Calibration using two laser trackers leica AT901 MR," Czech Technical University in Prague, Tech. Rep., 2014, http://clopema.felk.cvut.cz/files/reports/benes_laser_tracker.pdf. 4

[5] V. Petrík and V. Smutný, "Comparison of calibrations for the CloPeMa robot," Center for Machine Perception, K13133 FEE Czech Technical University, Prague, Czech Republic, Res. Rep. CTU–CMP–2014–01, Feb. 2014. 4

[6] J. Stria, D. Průša, V. Hlaváč, L. Wagner, V. Petrík, P. Krsek, and V. Smutný, "Garment perception and its folding using a dual-arm robot," in *Proc. Int. Conf. on Intelligent Robots and Systems (IROS)*, Chicago, Illinois, 2014, pp. 61–67. 4, 10

[7] "Radioactive Waste Robotic Sorter - RadioRoSo," 2016–2018, ECHORD++ Experiment. 4

[8] J. Maitin-Shepard, M. Cusumano-Towner, J. Lei, and P. Abbeel, "Cloth grasp point detection based on multiple-view geometric cues with application to robotic towel folding," in *Proc. IEEE Int. Conf. on Robotics and Automation (ICRA)*, 2010, pp. 2308–2315. 6, 7, 8

[9] Y. Li, D. Xu, Y. Yue, Y. Wang, S.-F. Chang, E. Grinspun, and P. K. Allen, "Regrasping and unfolding of garments using predictive thin shell modeling," in *Proc. IEEE Int. Conf. on Robotics and Automation (ICRA)*, 2015, pp. 1382–1388. 6, 9

[10] A. Ramisa, G. Alenya, F. Moreno-Noguer, and C. Torras, "Using depth and appearance features for informed robot grasping of highly wrinkled clothes,"

in *Proc. IEEE Int. Conf. on Robotics and Automation (ICRA)*, 2012, pp. 1703–1708. 6

[11] G. Alenyà Ribas, A. Ramisa Ayats, F. Moreno-Noguer, and C. Torras, "Characterization of textile grasping experiments," in *Proc. ICRA Workshop on Conditions for Replicable Experiments and Performance Comparison in Robotics Research*, 2012, pp. 1–6. 7

[12] Y. Kita and N. Kita, "A model-driven method of estimating the state of clothes for manipulating it," in *Proc. IEEE Workshop on Applications of Computer Vision (WACV)*, 2002, pp. 63–69. 7

[13] Y. Kita, F. Saito, and N. Kita, "A deformable model driven visual method for handling clothes," in *Proc. IEEE Int. Conf. on Robotics and Automation (ICRA)*, 2004, pp. 3889–3895. 7

[14] Y. Kita, T. Ueshiba, E. S. Neo, and N. Kita, "Clothes state recognition using 3D observed data," in *Proc. IEEE Int. Conf. on Robotics and Automation (ICRA)*, 2009, pp. 1220–1225. 8

[15] Y. Kita, E. S. Neo, T. Ueshiba, and N. Kita, "Clothes handling using visual recognition in cooperation with actions," in *Proc. Int. Conf. on Intelligent Robots and Systems (IROS)*, 2010, pp. 2710–2715. 8

[16] Y. Kita, F. Kanehiro, T. Ueshiba, and N. Kita, "Clothes handling based on recognition by strategic observation," in *IEEE-RAS Int. Conf. on Humanoid Robots (Humanoids)*, 2011, pp. 53–58. 8

[17] Y. Li, C.-F. Chen, and P. K. Allen, "Recognition of deformable object category and pose," in *Proc. IEEE Int. Conf. on Robotics and Automation (ICRA)*, 2014, pp. 5558–5564. 8

[18] J. Hu and Y. Kita, "Classification of the category of clothing item after bringing it into limited shapes," in *IEEE-RAS Int. Conf. on Humanoid Robots (Humanoids)*, 2015, pp. 588–594. 8

[19] L. Sun, S. Rogers, G. Aragon-Camarasa, and J. P. Siebert, "Recognising the clothing categories from free-configuration using gaussian-process-based interactive perception," in *Proc. IEEE Int. Conf. on Robotics and Automation (ICRA)*, 2016, pp. 2464–2470. 8

[20] F. Osawa, H. Seki, and Y. Kamiya, "Unfolding of massive laundry and classification types by dual manipulator." *J. Advanced and Intelligent Informatics (JACIII)*, vol. 11, no. 5, pp. 457–463, 2007. 8

[21] M. Cusumano-Towner, A. Singh, S. Miller, J. F. O'Brien, and P. Abbeel, "Bringing clothing into desired configurations with limited perception," in *Proc. IEEE Int. Conf. on Robotics and Automation (ICRA)*, 2011, pp. 3893–3900. 8, 9

[22] A. Doumanoglou, A. Kargakos, T.-K. Kimand, and S. Malassiotis, "Autonomous active recognition and unfolding of clothes using random decision forests and probabilistic planning," in *Proc. IEEE Int. Conf. on Robotics and Automation (ICRA)*, 2014, pp. 987–993. 8, 9

[23] H. Yuba, S. Arnold, and K. Yamazaki, "Unfolding of a rectangular cloth based on action selection depending on recognition uncertainty," in *IEEE/SICE Int. Symp. on System Integration (SII)*, Dec 2015, pp. 623–628. 9

[24] D. Triantafyllou, I. Mariolis, A. Kargakos, S. Malassiotis, and N. Aspragathos, "A geometric approach to robotic unfolding of garments," *Robotics and Autonomous Systems*, vol. 75, pp. 233 – 243, 2016. 9

[25] B. Willimon, S. Birchfield, and I. Walker, "Model for unfolding laundry using interactive perception," in *Proc. Int. Conf. on Intelligent Robots and Systems (IROS)*, 2011, pp. 4871–4876. 9

[26] L. Sun, G. Aragon-Camarasa, P. Cockshott, S. Rogers, and J. P. Siebert, "A Heuristic-Based Approach for Flattening Wrinkled Clothes," in *Annu. Conf. Towards Autonomous Robotic Systems (TAROS)*, 2013, pp. 148–160. 9

[27] L. Sun, G. Aragon-Camarasa, S. Rogers, and J. P. Siebert, "Accurate garment surface analysis using an active stereo robot head with application to dual-arm flattening," in *Proc. IEEE Int. Conf. on Robotics and Automation (ICRA)*, 2015, pp. 185–192. 9, 10

[28] Y. Li, X. Hu, D. Xu, Y. Yue, E. Grinspun, and P. K. Allen, "Multi-sensor surface analysis for robotic ironing," in *Proc. IEEE Int. Conf. on Robotics and Automation (ICRA)*, 2016, pp. 5670–5676. 9

[29] S. Miller, J. van den Berg, M. Fritz, T. Darrell, K. Goldberg, and P. Abbeel, "A geometric approach to robotic laundry folding," *Int. J. Robotics Research (IJRR)*, vol. 31, no. 2, pp. 249–267, 2012. 10

[30] S. Miller, M. Fritz, T. Darrell, and P. Abbeel, "Parametrized shape models for clothing," in *Proc. IEEE Int. Conf. on Robotics and Automation (ICRA)*, 2011, pp. 4861–4868. 10

[31] J. van den Berg, S. Miller, K. Y. Goldberg, and P. Abbeel, "Gravity-based robotic cloth folding." in *Int. Workshop on the Algorithmic Foundations of Robotics (WAFR)*, 2010, pp. 409–424. 11, 12

[32] Y. Li, Y. Yue, D. Xu, E. Grinspun, and P. K. Allen, "Folding deformable objects using predictive simulation and trajectory optimization," in *Proc. Int. Conf. on Intelligent Robots and Systems (IROS)*, 2015. 13, 14

[33] J. Bender, M. Muller, and M. Macklin, "Position-based simulation methods in computer graphics," *EUROGRAPHICS Tutorial Notes*, 2015. 13

[34] A. Dixit and H. S. Mali, "Modeling techniques for predicting the mechanical properties of woven-fabric textile composites: A review," *Mechanics of Composite Materials*, vol. 49, no. 1, pp. 1–20, 2013. 14, 18

[35] M. King, P. Jearanaisilawong, and S. Socrate, "A continuum constitutive model for the mechanical behavior of woven fabrics," *Int. J. of Solids and Structures*, vol. 42, no. 13, pp. 3867–3896, 2005. 15, 17

[36] F. T. Peirce, "The geometry of cloth structure," *J. Textile Institute Trans.*, vol. 28, no. 3, pp. T45–T96, 1937. 15

[37] S. Kawabata, M. Niwa, and H. Kawai, "The finite-deformation theory of plain-weave fabrics part i: The biaxial-deformation theory," *J. Textile Institute*, vol. 64, no. 1, pp. 21–46, 1973. 15

[38] P. Potluri, S. Ariadurai, and I. Whyte, "A general theory for the deformation behaviour of non-plain-weave fabrics under biaxial loading," *J. Textile Institute*, vol. 91, no. 4, pp. 493–508, 2000. 15

[39] X. Zeng, V. Tan, and V. Shim, "Modelling inter-yarn friction in woven fabric armour," *Int. J. Numerical Methods in Engineering*, vol. 66, no. 8, pp. 1309–1330, 2006. 15

[40] J. M. Kaldor, D. L. James, and S. Marschner, "Simulating knitted cloth at the yarn level," *ACM Transactions on Graphics (TOG)*, vol. 27, no. 3, p. 65, 2008. 15

[41] J. M. Kaldor, D. L. James, and S. Marschner, "Efficient yarn-based cloth with adaptive contact linearization," *ACM Transactions on Graphics (TOG)*, vol. 29, no. 4, p. 105, 2010. 15

[42] J. M. Kaldor, "Simulating yarn-based cloth," Ph.D. dissertation, Cornell University, 2011. 15, 16

[43] G. Cirio, J. Lopez-Moreno, D. Miraut, and M. A. Otaduy, "Yarn-level simulation of woven cloth," *ACM Transactions on Graphics (TOG)*, vol. 33, no. 6, p. 207, 2014. 16

[44] E. M. Parsons, T. Weerasooriya, S. Sarva, and S. Socrate, "Impact of woven fabric: Experiments and mesostructure-based continuum-level simulations," *J. Mechanics and Physics of Solids*, vol. 58, no. 11, pp. 1995–2021, 2010. 17

[45] E. M. Parsons, M. J. King, and S. Socrate, "Modeling yarn slip in woven fabric at the continuum level: Simulations of ballistic impact," *J. Mechanics and Physics of Solids*, vol. 61, no. 1, pp. 265–292, 2013. 17

[46] J. R. Collier, B. J. Collier, G. O'Toole, and S. Sargand, "Drape prediction by means of finite-element analysis," *J. Textile Institute*, vol. 82, no. 1, pp. 96–107, 1991. 17

[47] B. Chen and M. Govindaraj, "A physically based model of fabric drape using flexible shell theory," *Textile Research Journal*, vol. 65, no. 6, pp. 324–330, 1995. 17

[48] B. Chen and M. Govindaraj, "A parametric study of fabric drape," *Textile Research Journal*, vol. 66, no. 1, pp. 17–24, 1996. 17

[49] L. Gan, N. Ly, and G. Steven, "A study of fabric deformation using nonlinear finite elements," *Textile Research Journal*, vol. 65, no. 11, pp. 660–668, 1995. 17

[50] J. W. Eischen, S. Deng, and T. G. Clapp, "Finite-element modeling and control of flexible fabric parts," *IEEE Computer Graphics and Applications*, vol. 16, no. 5, pp. 71–80, 1996. 17, 18

[51] X. Man, "A mathematical and computational multiscale clothing modeling framework," Ph.D. dissertation, The University of Iowa, 2006. 18

[52] R. W. Williams, "Measuring and modeling the anisotropic, nonlinear and hysteretic behavior of woven fabrics," Ph.D. dissertation, University of Iowa, 2010. 18

[53] E. Oñate, "Thick/Thin plates. Reissner-Mindlin theory," in *Structural Analysis with the Finite Element Method Linear Statics: Vol. 2. Beams, Plates and Shells*. Dordrecht: Springer Netherlands, 2013, pp. 291–381. 18

[54] J. C. Simo and D. D. Fox, "On a stress resultant geometrically exact shell model. Part I: formulation and optimal parametrization," *Computer Methods in Applied Mechanics and Engineering*, vol. 72, no. 3, pp. 267–304, 1989. 18

[55] J. C. Simo, D. D. Fox, and M. S. Rifai, "On a stress resultant geometrically exact shell model. Part II: the linear theory; computational aspects," *Computer Methods in Applied Mechanics and Engineering*, vol. 73, no. 1, pp. 53–92, 1989. 18

[56] J. C. Simo, D. D. Fox, and M. S. Rifai, "On a stress resultant geometrically exact shell model. Part III: computational aspects of the nonlinear theory," *Computer Methods in Applied Mechanics and Engineering*, vol. 79, no. 1, pp. 21–70, 1990. 18

[57] F. Cirak, M. Ortiz, and P. Schroder, "Subdivision surfaces: a new paradigm for thin-shell finite-element analysis," *Int. J. Numerical Methods in Engineering*, vol. 47, no. 12, pp. 2039–2072, 2000. 18, 19

[58] B. Thomaszewski, M. Wacker, and W. Straßer, "A consistent bending model for cloth simulation with corotational subdivision finite elements," in *Proc. ACM SIGGRAPH/Eurographics Symp. on Computer Animation*, 2006, pp. 107–116. 19

[59] L. Noels and R. Radovitzky, "A new discontinuous Galerkin method for Kirchhoff–Love shells," *Computer Methods in Applied Mechanics and Engineering*, vol. 197, no. 33, pp. 2901–2929, 2008. 19

[60] L. Noels, "A discontinuous Galerkin formulation of non-linear Kirchhoff–Love shells," *Int. J. Numerical Methods in Engineering*, vol. 78, no. 3, pp. 296–323, 2009. 19

[61] P. Kaufmann, S. Martin, M. Botsch, E. Grinspun, and M. Gross, "Enrichment textures for detailed cutting of shells," *ACM Transactions on Graphics (TOG)*, vol. 28, no. 3, p. 50, 2009. 19

[62] P. Kaufmann, "Discontinuous galerkin FEM in computer graphics," Ph.D. dissertation, ETH Zurich, Switzerland, 2013. 19

[63] M. Müller and M. Gross, "Interactive virtual materials," in *Proc. Graphics Interface*, 2004, pp. 239–246. 19

[64] J. Kiendl, K.-U. Bletzinger, J. Linhard, and R. Wüchner, "Isogeometric shell analysis with Kirchhoff–Love elements," *Computer Methods in Applied Mechanics and Engineering*, vol. 198, no. 49, pp. 3902–3914, 2009. 19

[65] C. Zheng, "Cloth simulation by isogeometric analysis," Ph.D. dissertation, University of Iowa, 2013. 19

[66] J. Lu and C. Zheng, "Dynamic cloth simulation by isogeometric analysis," *Computer Methods in Applied Mechanics and Engineering*, vol. 268, pp. 475 – 493, Jan. 2014. 19

[67] V. Petrík, V. Smutný, P. Krsek, and V. Hlaváč, "Robotic Garment Folding: Precision Improvement and Workspace Enlargement," in *Annu. Conf. Towards Autonomous Robotic Systems (TAROS)*, Liverpool, 2015, pp. 204–215. 20

[68] V. Petrík, V. Smutný, P. Krsek, and V. Hlaváč, "Physics-Based Model of Rectangular Garment for Robotic Folding," in *Proc. Int. Conf. on Intelligent Robots and Systems (IROS)*, Daejeon, 2016. 20

[69] V. Petrík, V. Smutný, P. Krsek, and V. Hlaváč, "Accuracy of Robotic Elastic Object Manipulation as a Function of Material Properties," in *Int. Workshop on Modelling and Simulation for Autonomous Systems (MESAS)*, Rome, 2016. 20

A Robotic Garment Folding: Precision Improvement and Workspace Enlargement

Reprint of our paper *Robotic Garment Folding: Precision Improvement and Workspace Enlargement*, which was published in the proceedings of the 16th Towards Autonomous Robotic Systems conference, TAROS 2015.

Robotic Garment Folding: Precision Improvement and Workspace Enlargement

Vladimír Petrík[1,2], Vladimír Smutný[1], Pavel Krsek[1], and Václav Hlaváč[2]

[1] Center for Machine Perception, Department of Cybernetics,
Faculty of Electrical Engineering, Czech Technical University in Prague
{petrivl3,smutny,krsek}@cmp.felk.cvut.cz
[2] Czech Institute of Informatics, Robotics, and Cybernetics,
Czech Technical University in Prague
hlavac@ciirc.cvut.cz

Abstract. The trajectory performed by a dual-arm robot while folding a piece of garment was studied. The garment folding was improved by adopting here proposed novel circular folding trajectory, which takes the flexibility of the garment into account. The benefit lies in an increased folding precision. In addition, several relaxations of the folding trajectory were introduced, thus enlarging the working space of the dual-arm robot.

The new folding trajectory was experimentally verified and compared to the state-of-the-art methods. The advocated approach assumes that the folding trajectory and the robot arms constitute a closed kinematic chain. Closed loop planning techniques introduced recently enable planning of the folding task without solving the inverse kinematics in each planning step. This approach has favourable properties because the model used is extensible. For instance, it is possible to take into account the force/tension applied by the robot grippers to the held garment.

Keywords: gravity based folding, garment folding, closed kinematic chain planning

1 Introduction

Humans manipulate soft materials intuitively while getting dressed, lacing their shoes, bending a piece of paper or folding a garment. The garment folding is studied in this contribution. The mentioned manipulation tasks are difficult for robots because of the high degree of freedom allowed by the soft materials. This work improved and experimentally verified the garment folding.

The robotic garment manipulation can be divided into two consecutive operations: unfolding and folding. The unfolding precedes the folding; it starts from the garment in a random configuration and it finishes in the configuration in which the garment is spread flat on the table.

Both operations were studied, starting from the simplest case: towel folding [7]. The unfolding was studied by several researchers using either data-driven methods [2] or model-driven methods [3, 4] for the garment state recognition. The

data-driven method uses depth data in order to estimate the grasp position as well as the following action. The model-driven method operates on the 3D point cloud, fitting the precomputed mesh models of the garment to the observation. All the mentioned approaches manipulate the garment in the air and finish with the unfolded garment grasped in both arms. Additional operation needs to be performed in order to put the garment on the table, which might lead to it being wrinkled. It is possible to flatten a wrinkled garment by stroking it using a robot arm/gripper [13].

The folding operation assumes that the garment lies flat on the table with unknown garment pose. Miller et al. in [9, 8] demonstrated that the folding can be split into the individual folds while the garment pose is estimated for each fold separately. They used a parametrized shape model [9] for representing the garment. The garment features were used while computing the fold. The fold can be completed according to the gravity based folding approach [8], which divides the gripper trajectory into several straight line segments as shown in Fig. 2. The used polygonal model and features sensed/computed from it were extended. A significant speed-up by a factor of several tens was achieved [12, 11]. The novel solution for the garment-table segmentation was also proposed in [12] in order to make garment folding possible on a regular table.

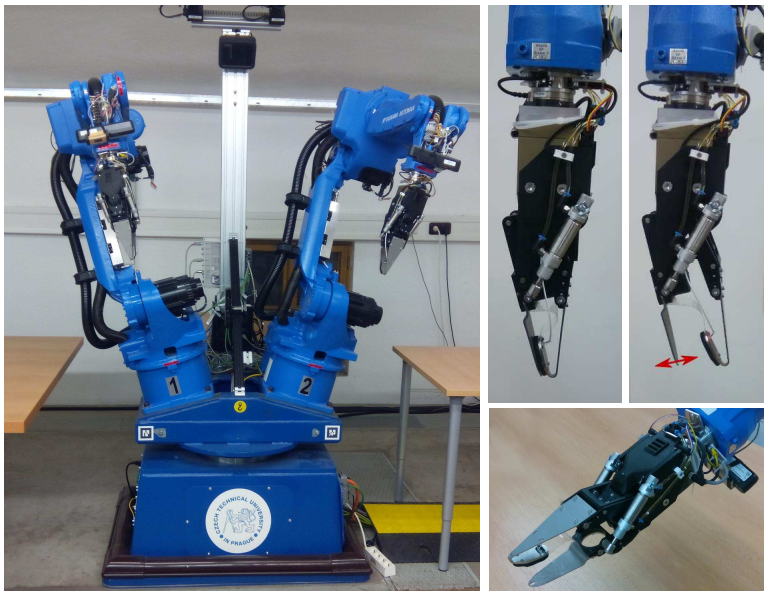

Fig. 1: CloPeMa dual-arm robot with grippers for garment manipulation. The grippers are compliant in the direction shown in the top right figure.

We propose an alternative strategy to the single gravity based fold. The robot trajectory for the fold execution is reformulated as the closed loop planning task,

which allows taking the garment flexibility into account. Several constraints relaxations, based on the garment flexibility, are described. Designed modifications were experimentally verified on the CloPeMa robot.

The CloPeMa robot, shown in Fig. 1, consists of two industrial welding robotic arms Yaskawa/Motoman MA1400 mounted on the torso. Its grippers were specially designed for the garment manipulation [6]. The grippers have variable stiffness which facilitates the grasping of the garment from a non-deformable table. The grippers have two asymmetrical fingers. A thin finger is used to slide under the garment, while the second finger incorporates various sensors.

This paper is structured as follows. Sec. 2 proposes the novel strategy for the single gravity based fold. Sec. 3 deals with the closed loop planning for the purpose of folding. Sec. 4 describes our experimental results. Sec. 5 concludes the paper and suggests future work.

2 Improvement of the Gravity Based Folding

The gravity based folding procedure [8] was built on several assumptions, of which the following are going to be examined in detail: *The garment has an infinite flexibility. Friction between the garment and the table surface is infinite.* These assumptions are not satisfied in the real environment, which leads to the garment sliding along the table surface while folding. Sliding of the garment leads to incorrectly overlapped parts of the folded garment as shown in Fig. 2. The sliding is worse for multiply folded garments because they become more rigid. By taking the flexibility into account, we designed a new trajectory as an alternative to the linear gravity based folding procedure [8].

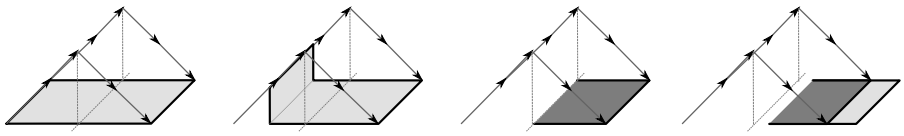

(a) Start state. (b) Folding. (c) Expected fold. (d) Incorrect fold.

Fig. 2: The linear gravity based folding and the garment sliding visualization. One fold is shown, starting from the start state and ending in the expected or the incorrect position. The success of the folding depends mostly on the garment flexibility and the friction between the garment and the table surface.

Let us assume the infinite friction between the table surface and the garment. Instead of the infinite flexibility of the whole garment, the following simplified model is considered. It is assumed that the material itself is rigid. The flexibility is expected in the folding line only. A circular folding trajectory along the folding straight line is the natural consequence of the assumption. In a frictionless case and a non-circular trajectory case, the material slides on the surface. The sliding

motion is caused by the varying distance between the gripper and the folding line, which results in pulling/pushing the garment along the table surface. The circular trajectory for one fold is shown in Fig. 3.

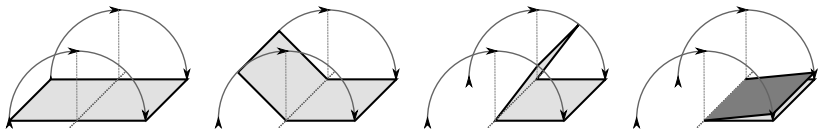

Fig. 3: The circular gravity based folding which preserves the constant distance between the grippers and the folding line.

Let us come back to the initial assumption, i.e. consider the infinitely flexible material and the infinite friction as in [8]. For the linear trajectory proposed in [8], the only reaction to the gravity force is exhibited by the grippers, which results in folding as shown in Fig. 2b. If the circular trajectory is considered, the garment bends due to the gravity force and additional reaction force caused by the friction. It results in applying the force in the direction of garment sliding. Due to the infinite friction the garment will not slide. When the friction force is smaller than the horizontal component of the gripper force, the sliding occurs resulting in the incorrect fold.

Both the infinitely flexible and the rigid materials are extreme models of the real world materials. The corresponding folding trajectories form boundaries of valid folding trajectories. The correct trajectory depends on the material properties and lies in between these limits as shown in Fig. 4d. In the finite friction case, the space of valid trajectories shrinks depending on the garment rigidity as well. In the original gravity based folding, the folding trajectory corresponds to the lower bound. We observed that the upper bound trajectory provides better folding results for real life garments. In the experimental section, both trajectories are tested on different garment types and compared in terms of the folding precision.

3 Closed Chain Garment Folding

The gravity based folding specifies the grasping point position unambiguously but the gripper orientation can vary while providing the correct fold. The possible gripper orientations while folding will be examined in this section.

3.1 Grasping and Folding

First, the folded garment needs to be grasped from the table surface. CloPeMa robot grippers were designed to slide one finger under the garment on the flat surface. The finger is compliant to reflect a small uncertainty in the table and the robot relative position. The grasping is shown in Fig. 5a. The whole trajectory

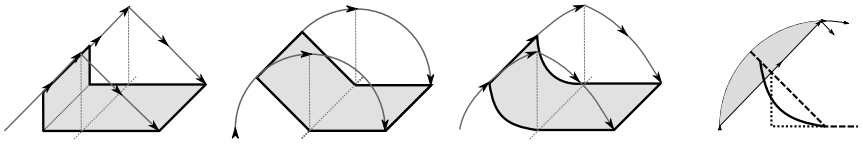

(a) Linear. (b) Circular. (c) General. (d) Side view.

Fig. 4: Possible folding trajectories bounded by linear and circular trajectories. Folding trajectories state space is visualized in gray in Fig. 4d, in which the garment position for the circular and linear folding is shown dashed and dotted, respectively. The general trajectory represents one of the trajectories from this state space.

including the grasping and the folding is shown in Fig. 5b. The grasping and folding trajectory defines a planning task. The required gripper orientation while grasping the garment constrains the space of achievable folding trajectories. A possible extension of the robot working space can be gained by relaxing the requirement of fixed gripper orientation. Let us introduce several relaxations.

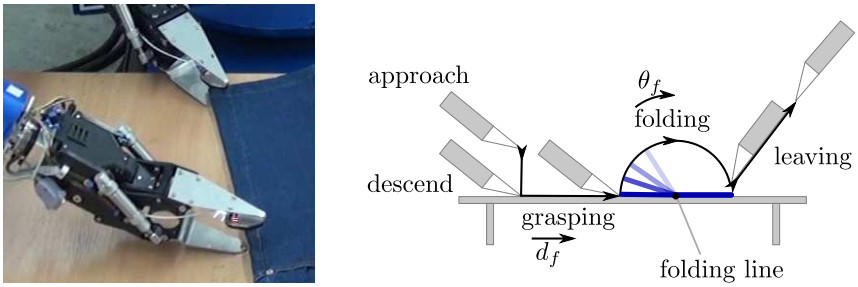

(a) Grasping with CloPeMa robot. (b) Individual fold steps.

Fig. 5: Grasping (a) and splitting the garment folding into steps. The diagram (b) reads from its left side in time. The shown grippers (a) are in the middle of the grasping step (b). The grippers open after the approaching step and close when the grasping step finishes. Variable d_f parametrizes the grasping step and variable θ_f parametrizes the folding step.

3.2 Azimuth Relaxation

We will focus on the grasping step, Fig. 5b, in which the only limitation is that the gripper's lower finger must be aligned with the table top. The orientation of the gripper in the horizontal plane can be arbitrary within the interval limited by the garment contour as shown in Fig. 6a. The angular offset δ_α reflects the angular dimension of the gripper finger tip. The value is constant and for the

grippers mounted on the CloPeMa robot it is set to 30°. This relaxation, named as the azimuth relaxation, is considered for the grasping phase only. During the fold, the relative orientation of the gripper and the held part of the garment has to be fixed not to crease the garment. Azimuth relaxation gives an additional degree of freedom per arm.

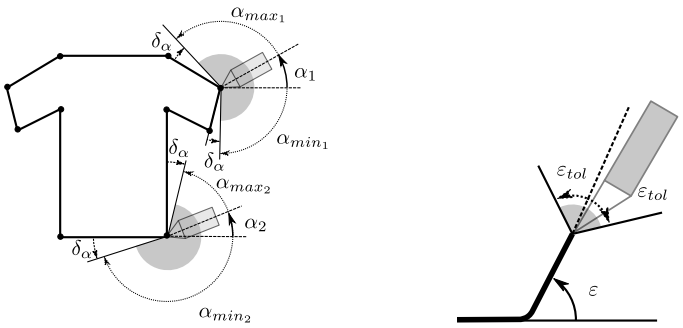

(a) Azimuth (b) Elevation

Fig. 6: Gripper constraints relaxation. The left drawing shows the azimuth relaxation limited by the garment contour. The right drawing shows the elevation relaxation limited by constant angles which depend on the garment flexibility.

3.3 Elevation Relaxation

The orientation of the gripper can be relaxed along the fold trajectory too. Instead of considering the fixed elevation angle (Fig. 6b), it could be relaxed slightly even for materials with low flexibility like jeans. The relaxation concerns the folding step only. For the grasping step, the elevation is determined by the allowed relative position of the table top and the gripper. A planning algorithm is used to find a feasible trajectory under the elevation relaxation.

3.4 Fold Planning by Solving the Inverse Kinematics

Let us start with the current fold planning procedure without relaxations. Trajectories, which grippers should follow, are parametrized in Cartesian space and then discretized using fixed-time steps. For each discretization step, the inverse kinematics (IK) is solved returning several robot configurations. The configuration of the robot should not change along the folding trajectory. The trajectory has to be collision free, too. If the set of solutions satisfying the above conditions is not empty, one of the solutions is selected. Otherwise, the fold is not accomplishable by the given robot.

The extended formulation, which deals with the relaxation, requires solving a planning task in a space of relaxed grippers positions. The IK is computed in each

step of the planner to obtain the robot position, which is checked for feasibility. The IK needs to be solved many times in this formulation. A computationally efficient IK is thus required. For 6 DOF arms, the closed form solver is often available but for redundant robots the IK has infinitely many solutions. CloPeMa robot is redundant with 13 degrees of freedom (DOF).

3.5 Fold Planning in Joint Space

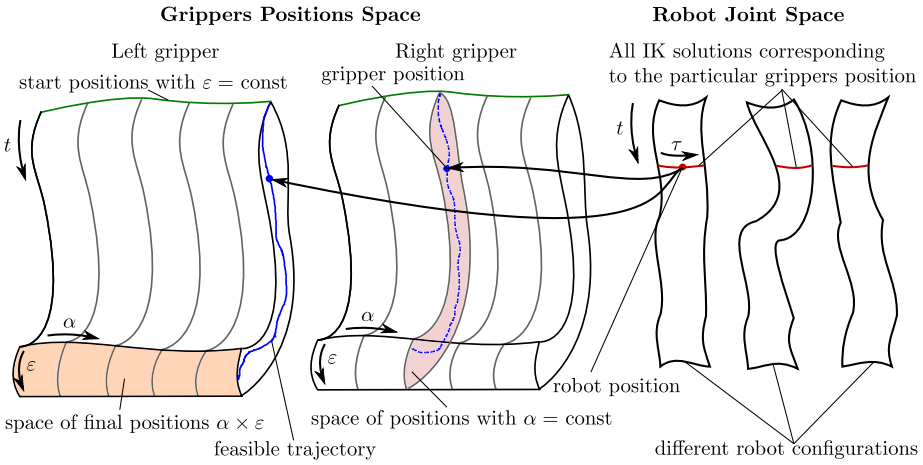

Fig. 7: The planning task for 13 DOF redundant robot with constraints relaxation. The leftmost two columns shows the left and right gripper positions space. The robot joint space is depicted on the right. The motion starts set (shown in green) has a fixed elevation ε but a relaxed azimuth α. Both azimuth and elevation are relaxed in the final position (light orange region). The time evolves roughly from top to bottom. A fixed azimuth is selected at the beginning of the motion. The manifold of the fixed azimuth is shown in light pink. Feasible trajectories (example shown in blue) never leave the manifold. The particular grippers position corresponds to a set of 1D curves (red) in the joint space as the grippers position has 12 DOF and robot has 13 joints. These curves can be parametrized, e.g. by the torso angle τ.

In order to avoid solving the inverse kinematics, the planner operates in joint coordinates. The randomized planning techniques like rapidly exploring random trees [5] are usually used but they require a valid state sampling algorithm. Unfortunately, the folding task forms a family of disjoint manifolds in the space of grippers positions. They are related to the manifolds in the joint space via the robot kinematics (Fig. 7). The probability to sample from the manifold approaches zero when a continuous state space is considered. The sampling on the manifold for the purpose of planning was studied in [10] where the closed

loop kinematics planning was considered as well. Reformulating the single fold to the closed loop kinematics form enables the use of the recently developed planning techniques like the planning by rapidly exploring manifolds [10] or the iterative relaxation of constraints [1].

The single fold together with grasping expressed in the kinematic model for the CloPeMa robot and circular gravity based folding is visualized in Fig. 8. Two closed loops are formed in frames structure while all relaxations described before are considered. Such a model is used for sampling the valid states as well as for planning using the CuikSuite software [10]. Different joint limits are used for each folding step (Fig. 5b), specifying kinematic restrictions of the manipulator and garment while sampling and planning. These limits form the complete fold task starting from garment grasping, through circular fold and ending in the release state where garment is not in the grippers. Relaxations are easily adjustable via joint limits to reflect different garment flexibility if necessary. The model is easily extensible if another relaxation is designed in the form of an additional joint. Note that the linear gravity based folding can be expressed as a closed loop kinematic planning task as well. The method does not require inverse kinematics which makes it more general.

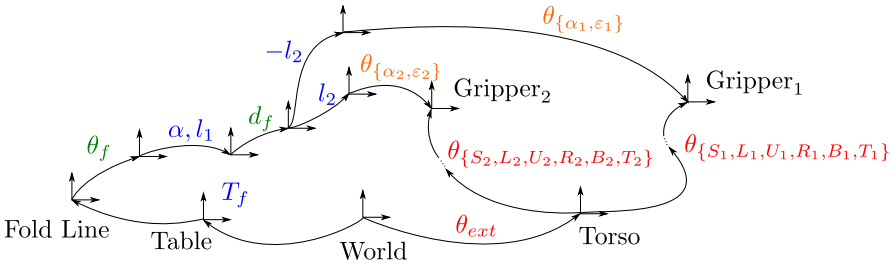

Fig. 8: The closed kinematic chain of the CloPeMa robot. Blue variables represent the position and parameters of the fold. They define a planning task. Red variables are individual joints of the robot. Orange color stands for the azimuth and elevation relaxations. The folding trajectory is parametrized by d_f and θ_f, respectively (Fig. 5b).

4 Experiments

4.1 Minimizing Folding Misalignment

The experiment measuring the displacement of the garment from the expected position compared the linear and the circular gravity based folding procedures. The experiment consists of the following steps: First, the garment is placed manually into the fixed position on the table. The fold is performed using one of the mentioned methods. The expected behavior is that the garment does not

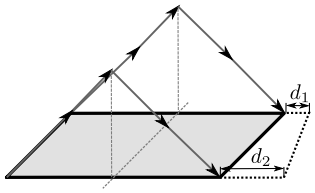

Fig. 9: The measurement of the garment displacement after incorrect fold. Dotted line represents the garment position after the fold is performed.

slide on the table and thus the non grasped edge of the garment will be in the same position after the fold. Due to the imprecise manipulation and the softness of the material, this is mostly not true. The displacement of the non grasped edge with respect to the expected position is measured as shown in Fig. 9. The displacements are zero for both d_1 and d_2 for the precise fold. The results of the experiments for different garments (Fig. 10) are shown in Tab. 1. Based on these results, it is clear that the circular folding outperformed the linear one in precision.

Table 1: Displacement (in millimeters) of the garment after the fold estimated from 5 folds per garment and per method. For jeans measurements, d_1 represents the leg opening offset and d_2 represents the waist offset. Displacements d_1 and d_2 were concatenated for the purpose of the towel statistics.

	Linear		Circular	
	mean	std	mean	std
Jeans_1 d_1	16.4	5.1	1.8	1.8
Jeans_1 d_2	32.8	4.8	0.8	1.8
Jeans_2 d_1	43.0	4.5	19.0	5.6
Jeans_2 d_2	32.6	4.3	6.0	0.7
Towel	14.3	2.1	7.0	4.5

(a) Jeans_1 (b) Jeans_2 (c) Towel

Fig. 10: The garments used for the experiment shown in the start state. The folding line is shown as dashed. The first and the second jeans differ in facing up and down only.

4.2 Workspace Enlargement

The next experiment deals with the workspace volume analysis for the purpose of the folding. The relaxations together with all active joints being used for the planning should enlarge the working space of the robot. The towel folding scenario with varying towel position is simulated to examine the working space of the CloPeMa robot.

The multidimensional workspace hyper volume is difficult to evaluate numerically. For demonstration purposes we have chosen to sample the working space along chosen axis while keeping other parameters constant. The results and the scenario are shown in Fig 11. Three different cases were investigated and in all cases the elevation relaxation was enabled. The first case shows the working space for fixed torso axis and for relaxed azimuth constraint with limits visualized in the left drawing. In the second case the torso axis was relaxed but the azimuth angle was fixed for both arms. Note that working space for the second case varies depending on the selected azimuth angles. From all the tested angles, we selected one producing the largest working space. The third case visualizes the possible positions when all the relaxations were allowed (i.e. elevation, azimuth, torso).

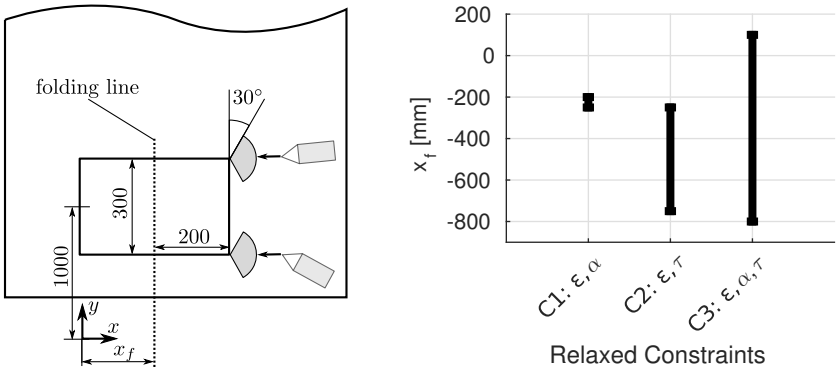

(a) Single fold scheme for towel (b) Succesfully planned fold positions

Fig. 11: Workspace analysis experiment with the torso axis located in the origin. The fold was planned for varying folding line position x_f. The range of x_f was investigated under different relaxations. In the first case, the elevation and the azimuth were relaxed. In the second case, only the elevation was relaxed but the torso motion was allowed. The last case considered the azimuth and elevation relaxations, as well as the torso motion.

Based on these results, it is clear that the space of possible towel locations is significantly larger when the relaxations are allowed. Asymmetrical results are caused by the fact that grasping and releasing positions of the gripper are not

symmetrical. Reachable distance of the robot is thus larger in the direction of folding.

The method generality and workspace enlargement is at the cost of longer computational time. The CuikSuite software valid states sampling takes several minutes compared to several seconds in the closed form inverse kinematics case. The computational cost can be overcome by another sampling technique or using the combination of planning approaches we mentioned. We will investigate these possibilities in the future.

5 Conclusions

This paper examined the planning of a single fold within the garment folding procedure performed by two robotic arms. It has been demonstrated that the originally proposed gravity based folding can be improved by the use of a circular trajectory, which is more suitable for real life garments. Experiments have been performed for several garment types using the CloPeMa robot, quantifying the improvement in terms of folding precision.

The next contribution concerned the size of the robot working space for the purpose of garment folding. We observed with the original linear folding trajectories that the working space is rather small even for bulky robotic arms like those of the CloPeMa robot. It was shown that constraints relaxation may extend the working space. Several relaxations have been introduced, with garment flexibility being taken into account.

Planning with relaxations has been studied, starting by extending the inverse kinematics based solution. Next, the closed kinematic chains have been proposed for the planning under relaxations and used to perform our experiments. It can be concluded that the constraints relaxation extends the robot working space significantly.

The results may be important for the future of robot garment folding because they can lead to smaller sized robots for the same working volume and the size of the manipulated garment.

In future work, the garment flexibility can be estimated in the course of the folding. The force/torque sensor mounted between the gripper and the robot flange (as in CloPeMa robot) or a fully force compliant robot as KUKA LBR can be used for the estimation. Based on such estimation, the relaxations limits can be updated online to provide the largest working space as well as a more precise fold. In such an extension, the folding trajectory will be replanned to reflect the properties of the previously unknown garment.

Acknowledgments. Thanks to Libor Špaček for discussions, proof reading and text corrections. This work was supported by the Technology Agency of the Czech Republic under Project TE01020197 Center Applied Cybernetics, the Grant Agency of the Czech Technical University in Prague, grant No. SGS15 /203/OHK3/3T/13 and the European Commission under the grant agreement FP7-ICT-288553.

References

1. Bayazit, O., Xie, D., Amato, N.: Iterative relaxation of constraints: a framework for improving automated motion planning. In: Intelligent Robots and Systems, 2005. (IROS 2005). 2005 IEEE/RSJ International Conference on. pp. 3433–3440 (Aug 2005)
2. Doumanoglou, A., Kargakos, A., Malassiotis, T.K.K.S.: Autonomous active recognition and unfolding of clothes using random decision forests and probabilistic planning. In: Proc. IEEE Int. Conf. on Robotics and Automation (ICRA). pp. 987–993 (2014)
3. Kita, Y., Kita, N.: A model-driven method of estimating the state of clothes for manipulating it. In: Proc. IEEE Workshop on Applications of Computer Vision (WACV). pp. 63–69 (2002)
4. Kita, Y., Ueshiba, T., Neo, E.S., Kita, N.: Clothes state recognition using 3D observed data. In: Proc. IEEE Int. Conf. on Robotics and Automation (ICRA). pp. 1220–1225 (2009)
5. Lavalle, S.M.: Rapidly-exploring random trees: A new tool for path planning. Tech. rep. (1998)
6. Le, T.H.L., Jilich, M., Landini, A., Zoppi, M., Zlatanov, D., Molfino, R.: On the development of a specialized flexible gripper for garment handling. Journal of Automation and Control Engineering 1(2), 255–259 (2013)
7. Maitin-Shepard, J., Cusumano-Towner, M., Lei, J., Abbeel, P.: Cloth grasp point detection based on multiple-view geometric cues with application to robotic towel folding. In: Proc. IEEE Int. Conf. on Robotics and Automation (ICRA). pp. 2308–2315 (2010)
8. Miller, S., van den Berg, J., Fritz, M., Darrell, T., Goldberg, K., Abbeel, P.: A geometric approach to robotic laundry folding. International Journal of Robotics Research (IJRR) 31(2), 249–267 (2012)
9. Miller, S., Fritz, M., Darrell, T., Abbeel, P.: Parametrized shape models for clothing. In: Proc. IEEE Int. Conf. on Robotics and Automation (ICRA). pp. 4861–4868 (2011)
10. Porta, J., Ros, L., Bohigas, O., Manubens, M., Rosales, C., Jaillet, L.: The CUIK Suite: Analyzing the Motion Closed-Chain Multibody Systems. Robotics & Automation Magazine, IEEE 21(3), 105–114 (2014), http://dx.doi.org/10.1109/mra.2013.2287462
11. Stria, J., Průša, D., Hlaváč, V., Wagner, L., Petrík, V., Krsek, P., Smutný, V.: Garment perception and its folding using a dual-arm robot. In: Intelligent Robots and Systems (IROS 2014), 2014 IEEE/RSJ International Conference on. pp. 61–67 (September 2014)
12. Stria, J., Průša, D., Hlaváč, V.: Polygonal models for clothing. In: Proc. Towards Autonomous Robotic Systems (TAROS) (August 2014)
13. Sun, L., Aragon-Camarasa, G., Cockshott, W.P., Rogers, S., Siebert, J.P.: A heuristic-based approach for flattening wrinkled clothes. In: Natraj, A., Cameron, S., Melhuish, C., Witkowski, M. (eds.) Towards Autonomous Robotic Systems - 14th Annual Conference, TAROS 2013, Oxford, UK, August 28-30, 2013, Revised Selected Papers. Lecture Notes in Computer Science, vol. 8069, pp. 148–160. Springer (2013)

B Physics-Based Model of Rectangular Garment for Robotic Folding

Reprint of our paper *Physics-Based Model of Rectangular Garment for Robotic Folding*, which will be published in the proceedings of the International Conference On Intelligent Robots and Systems, IROS 2016.

Physics-Based Model of Rectangular Garment for Robotic Folding

Vladimír Petrík[1], Vladimír Smutný[2], Pavel Krsek[1], Václav Hlaváč[1]

***Abstract*— The ability to perform an accurate robotic fold is essential to obtain the properly folded garment. Available solutions rely on a rough folding surface or on a comprehensive simulation, both preventing the garment from slipping on the table during folding. This paper proposes a new algorithm for a folding path design respecting the garment material properties and preventing the garment slipping. The folding path is derived based on the equilibrium of forces under the simplifying assumptions of a rectangular and homogeneous garment. This approach allows folding the rectangular garment on a low friction table surface as we demonstrated in the experiments performed by a dual-arm robotic testbed.**

I. Introduction

One of the skills in the robotic garment folding is an ability to perform a single fold. It involves the design of the robot gripper path, which folds the garment in the folding line as shown in Fig. 1. The robot gripper grasps the garment and follows planned path moving the garment into the required shape. If material properties are not considered in the design, the garment can slip on the folding surface, which later results in an inaccurate fold. The state-of-the-art methods of the folding path design assume the garment is infinitely flexible or rely on infinite friction between the folding surface and the garment. These assumptions proved to be unrealistic in practice and result in inaccurate folds.

This paper extends the previous works by assuming more realistic material properties. It leads to a more complex model so we restrict our study to rectangular garments only, but the proposed method can be generalised to more complex shapes. The assumptions neglect effects of dynamics and restrict the model to homogeneous rectangular garments with a constant bending stiffness. A physics-based garment model is used for computing the robot gripper path. The model is parametrised by a single parameter weight to stiffness ratio η. The method calculates the static equilibrium of forces in every state of the folding path.

The key contribution of the paper is the algorithm for a folding path design respecting the material properties. Our solution prevents the garment slipping on the horizontal folding surface and is able to fold the rectangular garment on a low friction table surface. We demonstrated the accuracy of our approach in a real robotic folding for different materials as well as for different folding surfaces.

[1]Vladimír Petrík, Pavel Krsek and Václav Hlaváč are with Czech Institute of Informatics, Robotics, and Cybernetics, Czech Technical University in Prague {vladimir.petrik, krsek, hlavac}@ciirc.cvut.cz

[2]Vladimír Smutný is with Faculty of Electrical Engineering, Czech Technical University in Prague smutny@fel.cvut.cz

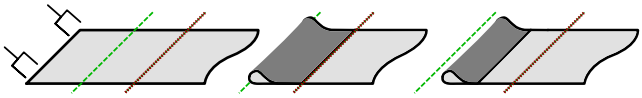

Fig. 1: Folding of a garment. The initial position is shown on the left side. The green dashed line represents the folding line, and the red dotted line represents the expected position of the grasped side of the garment. The robot grippers grasp the garment at one side only. Expected fold is shown in the middle, and inaccurate fold is shown on the right side. The inaccuracy is a result of incorrect manipulation, which causes the garment to slip or wrinkle. The folded garment shape near the folding line depends on the material properties. To visualise the slipping, the folding line is shown relatively to the robot while the expected side position is shown relatively to the garment. It means that the distance between lines changes if slipping occurs.

II. Related Work

The existing framework for the garment manipulation consists of bringing the garment to the initial state followed by the folding. The former assures the garment lies flat on the table and it was studied in [1], [2], [3], [4], [5]. The folding is decomposed into the individual folds, and the garment pose is estimated for each fold as shown in works [6], [7], [8].

The first approach for the design of the robotic garment folding path was shown by Berg et al. in [9]. Authors designed a gravity based folding path assuming infinitely flexible material and infinite friction between the garment and the folding surface. Such assumptions simplify the folding path significantly but are rarely met in a real environment. Note, that infinitely flexible garment has infinite weight to stiffness ratio η. The materials with very high η exist (e.g. chainmail), but they are rarely used for garments. Nevertheless, the path showed up to be a sufficient approximation if the requirements for folding accuracy were not high or if a table with high friction surface was used. The high friction surface is undesirable because it is difficult to flatten the garment on such a surface and it allows undesirable tensions in the folded garment. The resulting gripper path consists of a sequence of linear trajectories, and we will refer to this method as the linear gravity based folding.

To increase the precision while folding the real garment, Petrík et al. [10] designed a circular folding path. Instead of infinitely flexible garment, a rigid material with frictionless joint located in the folding line was assumed. The experimental comparison of the linear and circular folding was

provided when folding on the low friction table surface. The circular path achieved better folding accuracy for real garments (jeans, towel).

Another path for the folding was designed by Li et al. in [11]. Authors used a mass-spring model of the garment in an Autodesk Maya simulated environment. From several model parameters available in simulation, authors observed that shear resistance and friction coefficient is enough to model the garment folding. These parameters were tuned to match the real garment behaviour. For the gripper path, modelled by a Bézier curve, the resulting fold was evaluated virtually. The curve parameters were perturbed until a sufficiently good fold was obtained. Authors observed that their method is less stable when folding denim material (jeans, pants) due to the relatively high shear resistance.

III. Garment Model

In order to find the grippers folding path, a physics-based garment model is derived. The model is restricted by several assumptions, which respect the folding requirements and restrict the garment properties. One of the assumptions is that the garment material is modelled according to Euler-Bernoulli beam theory [12]. The theory describes the relation between external forces, an internal stress and a resulting shape. The approximations considered in the theory are valid for thin materials, such as garments. Furthermore, the garment is restricted to be rectangular, and material is assumed to be homogeneous, so the density and bending stiffness are constant. We also assumed that the folding line is parallel to the grasped side of the garment. It results in the folding as shown in Fig. 1. Under these assumptions, the garment can be represented in one dimension as shown in Fig. 2.

The model incorporates a contact of the garment with the table and a contact of the garment with the garment itself. The garment is in the partial contact with the table during the whole folding. The garment contact with itself occurs after the upper layer touches the lower layer of the garment. Considering these two contacts, we modelled the garment by four neighbouring sections. Two of these sections are hanging in free space and are modelled as strings. They are described by differential equations. The other sections are in contact, and they affect the boundary conditions of the strings. The state where both contacts occur is shown in Fig. 3.

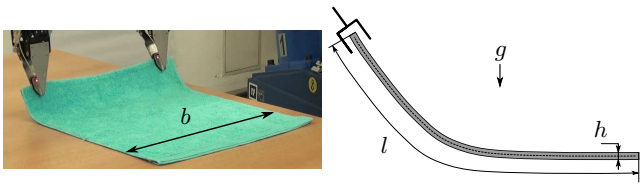

Fig. 2: A one-dimensional representation of the garment. A towel, with dimensions l, b, h, grasped by two grippers of a robot is shown on the left side. Its one-dimensional representation is shown on the right side. Symbol g shows the direction of a gravity force.

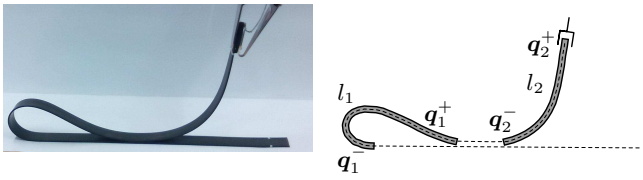

Fig. 3: The state of the model with both types of contacts: the contact between the garment and the folding surface, and between the garment itself. Two strings with length l_1 and l_2 are used to model this state. The effects of the contacts are incorporated into the string boundary conditions $\boldsymbol{q}_i$.

A. String Model

The string is supported on its ends only. The model of the string is derived based on the equilibrium of forces acting on an element $\mathrm{d}s$ of the string. The element and the acting forces are shown in Fig. 4. There is a tension force $T(s)$ acting in a direction of a tangent to the string at the position s. The angle between the tangent and the horizontal axis x is denoted by $\theta(s)$. A force perpendicular to tension force is called shear force and denoted by $V(s)$. Furthermore, the string bends under its own weight, which is expressed by a force $\rho_A\, b\, g\, \mathrm{d}s$, where b is the garment width, ρ_A stands for the material area density, and g is a gravitational acceleration. It is assumed the string is inextensible, and that the moment/curvature relation obeys the Euler-Bernoulli theorem [12]. For the string in equilibrium, the sum of forces must be zero which leads to the following equations:

$$\frac{\mathrm{d}}{\mathrm{d}s}\left(T(s)\cos\theta(s) + V(s)\sin\theta(s)\right) = 0\,, \tag{1}$$

$$\frac{\mathrm{d}}{\mathrm{d}s}\left(T(s)\sin\theta(s) - V(s)\cos\theta(s)\right) = \rho_A\, b\, g\,. \tag{2}$$

The sum of moments is zero as well, which leads to the relation between the shear force and the moment $M(s)$:

$$V(s) = \frac{\mathrm{d}M(s)}{\mathrm{d}s}\,. \tag{3}$$

The combination of the moment/curvature relation [12] and the angle/curvature relation [13] leads to:

$$\varkappa(s) = \frac{\mathrm{d}\theta(s)}{\mathrm{d}s} = \frac{M(s)}{K}\,, \tag{4}$$

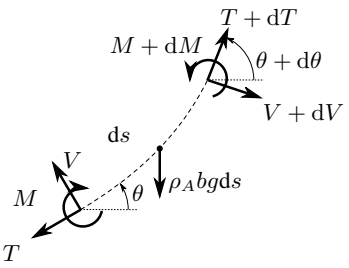

Fig. 4: The element of the string and the forces acting on it.

where $\varkappa(s)$ is the string curvature, and the constant K is introduced to represent the bending stiffness of the material. For isotropic materials without internal structure $K = E\,I$, where E represents Young's modulus and I is the second moment of area of the string cross-section. Neither E nor I have good meaning for the fabric materials. The linear relation is assumed in the moment/curvature relation. This is an approximation since the typical relation for the garment is nonlinear and often contains a hysteresis due to the internal friction. Combination of (3) and (4) results in:

$$V(s) = K\,\frac{\mathrm{d}^2\theta(s)}{\mathrm{d}s^2}\,. \tag{5}$$

The formulation is extended by the additional two equations representing the Cartesian position of the string elements:

$$\frac{\mathrm{d}x(s)}{\mathrm{d}s} = \cos\theta(s)\,, \qquad \frac{\mathrm{d}y(s)}{\mathrm{d}s} = \sin\theta(s)\,. \tag{6}$$

Let us introduce new variables:

$$\tilde{M}(s) = \frac{M(s)}{\rho_A\,b\,g}\,, \quad \tilde{V}(s) = \frac{V(s)}{\rho_A\,b\,g}\,, \quad \tilde{T}(s) = \frac{T(s)}{\rho_A\,b\,g}\,. \tag{7}$$

By substituting (5) and (7) into (1) and (2), we obtain:

$$\frac{\mathrm{d}}{\mathrm{d}s}\left(\tilde{T}(s)\cos\theta(s) + \frac{1}{\eta}\frac{\mathrm{d}^2\theta(s)}{\mathrm{d}s^2}\sin\theta(s)\right) = 0\,, \tag{8}$$

$$\frac{\mathrm{d}}{\mathrm{d}s}\left(\tilde{T}(s)\sin\theta(s) - \frac{1}{\eta}\frac{\mathrm{d}^2\theta(s)}{\mathrm{d}s^2}\cos\theta(s)\right) = 1\,, \tag{9}$$

where $\eta = \frac{\rho_A\,b\,g}{K}$ is the weight to stiffness ratio. The substitution (7) can be used because the robot controls the grippers position independently of the force required. After the substitution, the model depends on the weight to stiffness ratio only. If we need to know values of $M(s)$, $V(s)$ and $T(s)$, the constant K or ρ_A has to be measured in addition to η.

A system of the first order ordinary differential equations (ODE) is created from the higher order ODEs (8-9). A new variable representing the element state is introduced:

$$\boldsymbol{q}(s) = \left[\theta(s),\ \tilde{M}(s),\ \tilde{V}(s),\ \tilde{T}(s),\ x(s),\ y(s)\right]^\top\,. \tag{10}$$

The system of the first order ODEs is:

$$\frac{\mathrm{d}\boldsymbol{q}(s)}{\mathrm{d}s} = \begin{bmatrix} \eta\,q_2 \\ q_3 \\ -\cos q_1 + \eta\,q_2\,q_4 \\ \sin q_1 - \eta\,q_2\,q_3 \\ \cos q_1 \\ \sin q_1 \end{bmatrix}\,, \tag{11}$$

where q_i is the i-th element of the vector $\boldsymbol{q}(s)$.

B. Effect of Contacts

The contacts which occur during folding affect the boundary conditions of the strings. Two strings are used, which implies four boundaries in total. The boundaries for the first string are denoted:

$$\boldsymbol{q}_1(0) = \boldsymbol{q}_1^-\,, \qquad \boldsymbol{q}_1(l_1) = \boldsymbol{q}_1^+\,, \tag{12}$$

where superscript '$-$' denotes the left boundary condition and superscript '$+$' denotes the right boundary condition, similarly for the second string and other variables (T_1^-, θ_1^+, etc.). The contact of the garment with table affects only the left boundary condition of the first string (i.e. $\boldsymbol{q}_1^-$). The contact between the garment layers affects the boundary conditions $\boldsymbol{q}_1^+$ and $\boldsymbol{q}_2^-$ and causes the discontinuity between the strings.

The garment state is determined by state of all its elements $\boldsymbol{q}(s)$, for $s \in (0, l)$. Two garment state situations need to be distinguished during folding: the state, in which the contact between the lower and the upper layer does not exists (Fig. 5a and Fig. 5b) and the state where it does (Fig. 5c and Fig. 5d). In the former situation, only one string is modelled.

C. State of the Model

The garment model consists of two strings and individual states are distinguished by the boundary conditions. Fourteen conditions have to be specified in order to find a garment state. They restrict two times six first order ODEs (11) and two unknown lengths of the strings. Finding the solution leads to a boundary value problem [14]. More specifically, a multipoint boundary value problem is formed, and we used a tool [15] to solve it. The solver requires known limits of integration, and since lengths are not known a priori, we reformulate the string model into the dimensionless formulation. It was achieved by substitution $s = \varepsilon\,l$, where ε is a dimensionless position of the element.

The example of solving the garment state is shown for a completely folded state. The seven boundary conditions, which describe the folded state, are listed in the first column of Table I. The individual rows of the table correspond to equations representing the boundary conditions. For example, the first row for the first column of the table represents the boundary condition:

$$\theta_1^- = 180^\circ\,. \tag{13}$$

It means that the angle at the 'touchdown' point is restricted to be 180° in the folded state. Note, that boundary conditions are specified in such a way that the folded garment layers overlay. The length l can be easily adjusted, if different folding is desired (e.g. as in Fig. 1).

IV. Folding Path

The individual states of the model are determined by the boundary conditions. The boundary conditions specify the folding task by considering the restrictions of geometry and applied forces. For example, one of the conditions restricts the moment to be zero at the beginning of the first section ($\tilde{M}_1^- = 0$). Evolution of the garment states is called the garment path and denoted by:

$$\boldsymbol{q}(s,\tau)\,, \quad \tau \in (0, 1\rangle\ , \tag{14}$$

where τ is a dimensionless monotonic function of time. The whole folding time is specified manually. It has to be large enough so that the effect of dynamics can be neglected.

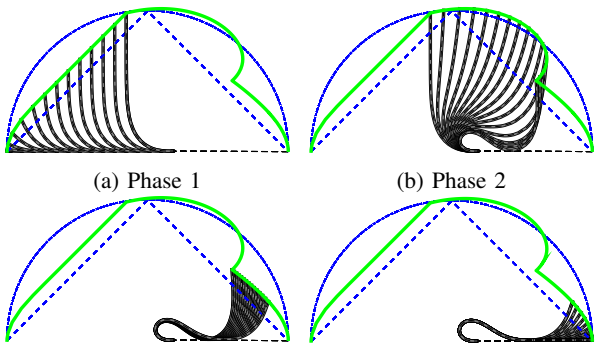

(a) Phase 1 (b) Phase 2

(c) Phase 3 (d) Phase 4

Fig. 5: Individual folding phases. The linear / circular path is shown in blue color.

While folding, four groups of states are distinguishable, and we call them folding phases. The individual phases are shown in Fig. 5. The garment states in a phase are determined by the constant boundary conditions except one, which we will call a control variable $\delta_i(\tau)$. The control variable $\delta_i(\tau)$ is a monotonic function of τ during the Phase i.

In the Phase 1, the garment is lifted up until its 'touchdown' point reaches the expected position, which was computed from the folded state. The Phase 2 bends the garment until the contact between the garment layers occurs. In the first two phases, there is no contact between the garment layers and thus only the second string is modelled. The contact introduces another seven conditions for the first string, and it is examined in the Phase 3 and Phase 4. In the former case, there is one point contact only, and the point of the contact moves in the direction of folding. The point of the contact is rolling without sliding. At the end of the Phase 3, the first string reaches its final shape. In the Phase 4, the second string is put on the lower layer until its length is zero.

Some of the boundary conditions depend on the values computed in a specific phase. For example, the expected position of the touchdown point is determined by the folded garment state. The phases are thus solved in the mixed order. First, the folded state is solved followed by the phases solving in order: 1, 4, 3, 2. It ensures that all required values are known before solving the phase. The Phase 3 and Phase 4 are solved backwards in time.

a) Folded State: Only the first string is modelled in the folded state. The boundary conditions ensure that the string is supported by the table at the beginning of the string and by the lower layer at the end of the string. The constants $\frac{3h}{2}$ and $\frac{h}{2}$ appear because the string model represents a neutral axis. The neutral axis is in the middle of the string due to the assumption of constant density and the rectangular shape. The constant h is negligible unless multiple folds are stacked.

b) Phase 1: The garment path starts from a state, in which the garment lies on the table and with the second string length equals to zero. The length of the string then increases linearly with time, which results in the garment lifting. During the lifting, the touchdown point is moving in the direction of folding. The lifting continues until the touchdown point reaches its final position, which was computed in advance based on the folded state of the garment. The variable δ_1 varies from 0 to $x_1^-(\tau_e)$, where τ_e represents the end of the folding and $x_1^-(\tau_e)$ is the boundary value of the folded state.

TABLE I: The boundary conditions for the individual folding phases. The symbol $\times$ represents that variable is not constrained. The symbol | indicates that the string is not modelled. The symbol δ_i parametrizes the Phase i.

	Folded State	Phase 1	Phase 2	Phase 3	Phase 4
θ_1^-	$180°$	|	|	$180°$	|
$\tilde{M}_1^-$	0	|	|	0	|
$\tilde{V}_1^-$	$\times$	|	|	$\times$	|
$\tilde{T}_1^-$	0	|	|	$\times$	|
x_1^-	$l + l_1 - x_1^+$	|	|	$x_1^-(\tau_e)$	|
y_1^-	$\frac{h}{2}$	|	|	$\frac{h}{2}$	|
θ_1^+	0	|	|	0	|
$\tilde{M}_1^+$	$\times$	|	|	$\times$	|
$\tilde{V}_1^+$	$\times$	|	|	$\times$	|
$\tilde{T}_1^+$	$\times$	|	|	$\times$	|
x_1^+	$\times$	|	|	$\times$	|
y_1^+	$\frac{3h}{2}$	|	|	$\frac{3h}{2}$	|
θ_2^-	|	$180°$	$180°$	0	0
$\tilde{M}_2^-$	|	0	0	$\tilde{M}_1^+$	0
$\tilde{V}_2^-$	|	$\times$	$\boldsymbol{\delta_2(\tau)}$	$\tilde{V}_1^+ - \boldsymbol{\delta_3(\tau)}$	$\times$
$\tilde{T}_2^-$	|	0	$\times$	$\tilde{T}_1^+$	0
x_2^-	|	l_2	$x_1^-(\tau_e)$	x_1^+	$l - l_2$
y_2^-	|	$\frac{h}{2}$	$\frac{h}{2}$	$\frac{3h}{2}$	$\frac{3h}{2}$
θ_2^+	|	$\times$	$\times$	$\times$	$\times$
$\tilde{M}_2^+$	|	0	0	0	0
$\tilde{V}_2^+$	|	$\times$	$\times$	$\times$	$\times$
$\tilde{T}_2^+$	|	$\times$	$\times$	$\times$	$\times$
x_2^+	|	$\times$	$\times$	$\times$	$\times$
y_2^+	|	$\times$	$\times$	$\times$	$\times$
l_1	$\times$	|	|	$\times$	|
l_2	|	$\boldsymbol{\delta_1(\tau)}$	$x_1^-(\tau_e)$	$x_1^-(\tau_e) - l_1$	$\boldsymbol{\delta_4(\tau)}$

c) Phase 2: In Phase 2, the garment should rather bend than be lifted. The length of the lifted section is fixed. The shear force V_2^- controls Phase 2, as we observed it is increasing monotonically during this phase. The shear force is increasing until the upper layer touches the lower layer of the garment. The control variable δ_2 varies from value $V_2^-(\tau_{1e})$ to $V_1^-(\tau_{3s})$, where τ_{1e} represents the end of the Phase 1 and τ_{3s} represents the start of the Phase 3. The value of $V_1^-(\tau_{3s})$ is known from the Phase 3.

d) Phase 3: In Phase 3, there is a point contact between the lower and the upper layer of the garment. The contact results in a discontinuity between the shear forces V_1^+ and V_2^-. The control variable δ_3 represents this discontinuity. The range of the control variable is from value $V_1^+(\tau_{4s}) - V_2^-(\tau_{4s})$ to 0. In Phase 3, only a single point of the upper layer is in the contact. The position of this point changes with the control variable.

e) Phase 4: The last phase represents the lowering of the garment. The first string reached the equilibrium and does not move in this phase. The control variable δ_4 represents

the length of the second string varying from 0 to its maximal length computed as $l - x_1^+(\tau_e)$. The last state of this phase is equal to the folded garment state.

The garment path is obtained by concatenating the states of the individual phases. The folding path is extracted from garment path directly. Only the position and orientation of the end of the string is used, which means that the robot is controlled by the position/orientation.

V. Experiments

We performed the experiment measuring the quality of the single fold for various garment materials and folding surfaces. The quality of the fold is measured based on the slipping of the lower layer from its initial position and based on the displacement of the planned and real position of the grasped side of the folded garment. The signed displacement is used in a way that positive values are used if the grasped side extends beyond the planned position (Fig. 6).

The weight to stiffness ratio was not known exactly and was estimated by the operator. The estimation was based on the maximal height of the manually folded garment (Fig. 6). The relation between the ratio η and the maximal height h_m (Fig. 7) was obtained by the simulation of the folded state. In the experiment, the garment was folded manually by the operator and the maximal height was measured. The manual fold uses the gravity for the garment bending similarly to the robotic folding. No additional force was used to deform the folded shape. The effect of the non-modelled deformation caused by the internal friction is thus minimised during the weight to stiffness estimation. The weight to stiffness ratio was then estimated from the experimentally obtained relation (Fig. 7).

Two folding surfaces were used: a melamine faced chipboard table surface and a table covered by a rough tablecloth. Furthermore, two shapes of garments were used: narrow strips and real rectangular garments - towels. The properties of the used materials are shown in Table. II.

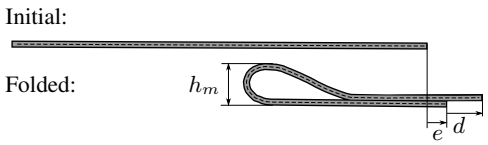

Fig. 6: The displacement measurement. The slippage e and the displacement d measure the quality of the fold and the maximal height h_m is used to estimate the material property.

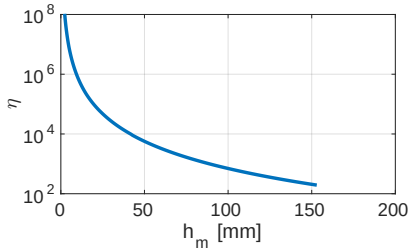

Fig. 7: The relation between the maximum height h_m and the weight to stiffness ratio η.

TABLE II: The properties of used materials. The lengths l, b, h are garment dimensions. The symbol h_m represents the maximal height of the folded garment and symbols ρ_A, K and η stand for material properties.

	l / b / h [mm]	h_m [mm]	ρ_A [kgm^{-2}]	K [Nm^2]	η [m^{-3}]
synthetic	525 / 57 / 1	10	0.75	$5.3{\cdot}10^{-7}$	800000
denim	525 / 110 / 1	30	0.70	$2.6{\cdot}10^{-5}$	30000
rubber1	995 / 36 / 3	70	3.95	$5.9{\cdot}10^{-4}$	2400
rubber2	995 / 59 / 4	89	5.25	$2.7{\cdot}10^{-3}$	1150
rubber3	995 / 50 / 5	99	6.55	$3.9{\cdot}10^{-3}$	850
towel1	590 / 360 / 1	24	0.30	$1.9{\cdot}10^{-5}$	58000
towel2	560 / 490 / 2	28	0.60	$7.6{\cdot}10^{-5}$	38500

A. Narrow Strips

The narrow strips were folded by one gripper only. Two fabrics were used for the strips: synthetic and denim. Furthermore, the strips with lower weight to stiffness ratio η were used: a Ethylene Propylene Diene Monomer rubbers with various thicknesses. Different thickness of the strips represents the different η in the experiment. Since the friction between the rubber and the table is large, we also conducted experiments with the paper sheet inserted between the rubber and the folding surface and denoted them as table/paper surface. Strips slide on the paper-table interface if horizontal force is larger than friction force between the paper and the table surface. The measured results are shown in the upper part of Table III.

Table III indicates that there is a relation between the slippage and displacement of the linear folding path and the surface friction. The lower slippages/displacements were measured for the higher friction. Furthermore, the lower weight to stiffness ratio results in the higher slippage/displacement

TABLE III: The measured lower layer slippage e and the measured layers displacement d. The upper part of the table shows the displacements for the narrow strips and the rest shows displacements for the real garments. The garments are ordered based on the weight to stiffness ratio η. The measured static friction coefficient is denoted by μ.

Surface	Garment	μ [-]	Slippage [mm] / Displacement [mm] Folding path		
			Linear	Circular	Our Model
table	synthetic	0.20	6 / -24	-10 / 46	**0 / -5**
	denim	0.26	15 / -28	-14 / 40	**0 / -1**
	rubber1	0.57	31 / -46	-21 / 68	**0 / -2**
	rubber2	0.57	28 / -45	-18 / 47	**0 / 4**
	rubber3	0.57	30 / -50	-11 / 32	**0 / 5**
table/paper	rubber1	0.31	39 / -55	-32 / 62	**0 / -3**
	rubber2	0.31	64 / -82	-35 / 53	**0 / 3**
	rubber3	0.31	70 / -91	-24 / 37	**0 / 5**
tablecloth	synthetic	0.53	0 / -19	0 / 31	**0 / -7**
	denim	0.81	0 / -10	0 / 28	**0 / -4**
	rubber1	0.80	23 / -42	-8 / 43	**0 / -2**
	rubber2	0.80	25 / -46	-8 / 39	**0 / 2**
	rubber3	0.80	30 / -50	-5 / 22	**0 / 3**
table	towel1	0.28	17 / -35	-10 / 56	**0 / 5**
	towel2	0.24	28 / -40	-10 / 43	**0 / 3**
tablecloth	towel1	1.23	0 / -23	0 / 41	**0 / 4**
	towel2	1.20	0 / -25	0 / 30	**0 / 3**

as well. This fulfils the expectation of the linear folding path as it was designed for infinitely flexible garments (infinite η) and for infinite surface friction. Based on the oriented displacements, it can be concluded that linear folding path has tendency to push the garment in the direction of folding.

On the contrary, the circular path tends to pull the garment. The circular folding path outperformed the linear path in the situations with low η only.

Our model based path outperformed both state-of-the-art methods: the linear as well as the circular folding path. For our path, there is no relation between the friction and the measured displacement in the experiment. It is a result of minimization of the horizontal force, which prevents the slipping of the garment in the most cases. We did not observed any slipping in the experiment.

B. Real Rectangular Garments

Two real towels were folded in order to show that the model is sufficient for rectangular garments folded by two grippers. The towel was grasped by its corners as shown in Fig. 1. A single folding path was designed using our one dimensional representation and this path was followed by both grippers simultaneously. We observed that the model error is negligible small, when folding with two grippers. The measured results are shown in the lower part of Table III. The errors are similar to strips folding: the linear path outperformed the circular path and the displacement of the linear folding can be lowered by the higher friction. Our folding path outperformed both of them. The results indicate that our folding path can be used, when folding rectangular garment with a dual arm robot without explicitly modelling of two dimensions.

C. Performance Evaluation

The performance of our method depends on the number of states computed for the path. The garment path displayed in Fig. 5 consists of 60 garment states with gripper positions approximately 20 mm apart and it was computed in 13 seconds. The computation was performed in MATLAB on Intel(R) Core(TM) i7-4610M CPU 3.00GHz.

VI. Conclusion

This paper examined the folding of the garment performed by the robotic arms. The folding path was designed respecting the material properties but restricting the garment to rectangular shape only. The designed path prevents the garment from slipping when folded on the low friction surface, which results in a better folding accuracy. The main advantage of our method is an ability to fold the garment on the table without using high friction folding surface. We performed experiments for several garments and folding surfaces, comparing our folding path with two state-of-the-art methods for folding path design. Our folding path outperformed the state-of-the-art methods in term of the precision and it was experimentally shown that it could be used for folding on the low friction table surface. It has been demonstrated that the folding path design cannot ignore the garment material properties. The experiments show that violations of our model assumptions by real garments do not result in inaccurate folds.

The reported work considered the folding of the homogeneous, rectangular shape garments only. In the future work, the rectangular shape assumption should be relaxed which will extend the set of the modelled garments. An extension to the non-rectangular shape could be achieved by simulating shell models instead of strings. We also assumed the material properties are known or are measured in advance by the operator. In future, these properties can be estimated in the course of the folding by using the camera recognising the garment shape during the folding.

Acknowledgment

This work was supported by the Technology Agency of the Czech Republic under Project TE01020197 Center Applied Cybernetics, the Grant Agency of the Czech Technical University in Prague, grant No. SGS15/203/OHK3/3T/13.

References

[1] D. Triantafyllou, I. Mariolis, A. Kargakos, S. Malassiotis, and N. Aspragathos, "A geometric approach to robotic unfolding of garments," *Robotics and Autonomous Systems*, vol. 75, pp. 233 – 243, 2016.

[2] A. Doumanoglou, A. Kargakos, T.-K. Kimand, and S. Malassiotis, "Autonomous active recognition and unfolding of clothes using random decision forests and probabilistic planning," in *Proc. IEEE Int. Conf. on Robotics and Automation (ICRA)*, 2014, pp. 987–993.

[3] Y. Kita, T. Ueshiba, E. S. Neo, and N. Kita, "Clothes state recognition using 3D observed data," in *Proc. IEEE Int. Conf. on Robotics and Automation (ICRA)*, 2009, pp. 1220–1225.

[4] Y. Kita and N. Kita, "A model-driven method of estimating the state of clothes for manipulating it," in *Proc. IEEE Workshop on Applications of Computer Vision (WACV)*, 2002, pp. 63–69.

[5] J. Maitin-Shepard, M. Cusumano-Towner, J. Lei, and P. Abbeel, "Cloth grasp point detection based on multiple-view geometric cues with application to robotic towel folding," in *Proc. IEEE Int. Conf. on Robotics and Automation (ICRA)*, 2010, pp. 2308–2315.

[6] S. Miller, M. Fritz, T. Darrell, and P. Abbeel, "Parametrized shape models for clothing," in *Proc. IEEE Int. Conf. on Robotics and Automation (ICRA)*, 2011, pp. 4861–4868.

[7] S. Miller, J. van den Berg, M. Fritz, T. Darrell, K. Goldberg, and P. Abbeel, "A geometric approach to robotic laundry folding," *International Journal of Robotics Research (IJRR)*, vol. 31, no. 2, pp. 249–267, 2012.

[8] J. Stria, D. Průša, V. Hlaváč, L. Wagner, V. Petrík, P. Krsek, and V. Smutný, "Garment perception and its folding using a dual-arm robot," in *Proc. Int. Conf. on Intelligent Robots and Systems (IROS)*, 2014, pp. 61–67.

[9] J. van den Berg, S. Miller, K. Y. Goldberg, and P. Abbeel, "Gravity-based robotic cloth folding." in *Int. Workshop on the Algorithmic Foundations of Robotics (WAFR)*, 2010, pp. 409–424.

[10] V. Petrík, V. Smutný, P. Krsek, and V. Hlaváč, "Robotic Garment Folding: Precision Improvement and Workspace Enlargement," in *Annu. Conf. Towards Autonomous Robotic Systems (TAROS)*, 2015, pp. 204–215.

[11] Y. Li, Y. Yue, D. Xu, E. Grinspun, and P. K. Allen, "Folding deformable objects using predictive simulation and trajectory optimization," in *Proc. Int. Conf. on Intelligent Robots and Systems (IROS)*. IEEE/RSJ, 2015.

[12] S. Timoshenko, *History of strength of materials*. New York: McGraw-Hill, 1953.

[13] E. Kreyszig, *Differential Geometry*. New York: Dover, 1991.

[14] R. E. Bellman and R. E. Kalaba, "Quasilinearization and nonlinear boundary-value problems," RAND Corporation, Santa Monica, Tech. Rep., 1965.

[15] J. A. Kierzenka and L. F. Shampine, "A bvp solver that controls residual and error," *J. Numer. Anal. Ind. Appl. Math (JNAIAM)*, pp. 1–2, 2008.

C Accuracy of Robotic Elastic Object Manipulation as a Function of Material Properties

Reprint of our paper *Accuracy of Robotic Elastic Object Manipulation as a Function of Material Properties*, which will be published in the proceedings of the International Workshop on Modelling and Simulation for Autonomous Systems, MESAS 2016.

Accuracy of Robotic Elastic Object Manipulation as a Function of Material Properties

Vladimír Petrík[1], Vladimír Smutný[2], Pavel Krsek[1], and Václav Hlaváč[1]

[1] Czech Institute of Informatics, Robotics, and Cybernetics,
Czech Technical University in Prague
{vladimir.petrik,krsek,hlavac}@ciirc.cvut.cz
[2] Center for Machine Perception, Department of Cybernetics, Faculty of Electrical Engineering
Czech Technical University in Prague
smutny@cmp.felk.cvut.cz

Abstract. We deal with the problem of thin string (1D) or plate (2D) elastic material folding and its modeling. The examples could be metallic wire, metal, kevlar or rubber sheet, fabric, or as in our case, garment. The simplest scenario attempts to fold rectangular sheet in the middle. The quality of the fold is measured by relative displacement of the sheet edges. We use this scenario to analyse the effect of the inaccurate estimation of the material properties on the fold quality. The same method can be used for accurate placing of the elastic sheet in applications, e.g. the industrial production assembly.

In our previous work, we designed a model simulating the behavior of homogeneous rectangular garment during a relatively slow folding by a dual-arm robot. The physics based model consists of a set of differential equations derived from the static forces equilibrium. Each folding phase is specified by a set of boundary conditions. The simulation of the garment behavior is computed by solving the boundary value problem. We have shown that the model depends on a single material parameter, which is a weight to stiffness ratio. For a known weight to stiffness ratio, the model is solved numerically to obtain the folding trajectory executed by the robotic arms later.

The weight to stiffness ratio can be estimated in the course of folding or manually in advance. The goal of this contribution is to analyse the effect of the ratio inaccurate estimation on the resulting fold. The analysis is performed by simulation and in a real robotic garment folding using the CloPeMa dual-arm robotic testbed. In addition, we consider a situation, in which the weight to stiffness ratio cannot be measured exactly but the range of the ratio values is known. We demonstrate that the fixed value of the ratio produces acceptable fold quality for a reasonable range of the ratio values. We show that only four weight to stiffness ratio values can be used to fold all typical fabrics varying from a soft (e.g. sateen) to a stiff (e.g. denim) material with the reasonable accuracy. Experiments show that for a given range of the weight to stiffness ratio one has to choose the value on the pliable end of the range to achieve acceptable results.

Keywords: robotic soft material folding, physical elastic flat material model, robotic fold accuracy

1 Introduction

The robotic manipulation with the soft material remains a challenging task due to the high degree of freedom of the soft material. One of the studied manipulation skills is the ability to fold the material accurately. The folding requires a folding trajectory which depends on several material properties. Estimation of these properties is inaccurate or omitted in real environment and then the folding itself is inaccurate as well. The folding inaccuracy as a function of the material properties is studied in this contribution.

The fold is specified by the folding line as shown in Fig. 1. The folding line divides the sheet into two parts. The goal of the folding is to move the left part on the top of the right part. The folding is achieved by following the folding trajectory. In the simplest scenario, the folding is aligned with the sheet edges and divides the sheet into two equally sized parts (Fig. 1). In this paper, all performed experiments assume the simplest scenario. The correct folding in the simplest scenario results in aligned edges of the sheet. The quality of the fold can be quantified by the distance between edges, which is zero if folding was accurate.

The goal of this paper is to analyse the fold quality for different robotic folding methods. In robotic folding, the folding trajectory is generated for the given sheet properties. The folding trajectory starts with grasping of the one side of garment while the opposite side lies freely on the folding surface. The trajectory depends on several sheet properties, for instance the size, density and stiffness. Generated trajectory is used to perform the folding by a robot. If the unsuitable trajectory is generated, the resulting fold is inaccurate. In practice, the sheet properties are measured or estimated in advance. The estimation might be inaccurate and the designed trajectory is thus unsuitable for the real material. In the following two sections, the methods used for generation of the folding trajectory are described. The rest of the paper examines several experiments performed both in simulation and in real robotic testbed. These experiments analyze the effect of the properties estimation inaccuracy on the resulting fold.

The key contribution of the paper is a methodology, which select a folding trajectory for a given range of the material properties. This trajectory provides the satisfactory folding results for all materials from a given range. It also gives a possibility to precompute the trajectories and thus provides a fast planning algorithm for the folding trajectory design. This is demonstrated for all typical fabrics used for garments, where we will show that only four trajectories are required to fold all fabrics.

2 Related Work

To the author's knowledge, there are four different approaches for the folding trajectory design. Two of them are independent of material properties and the trajectory is described by a set of simple curves. The other two approaches depend on the material properties and are planned based on simulation.

The first approach for trajectory design is gravity based folding method [2], denoted as linear trajectory hereinafter. The trajectory shape was derived assuming the infinitely flexible material and infinite friction between the garment and the folding surface. Such assumptions are unrealistic and lead to imprecise fold as shown in work [6], where the

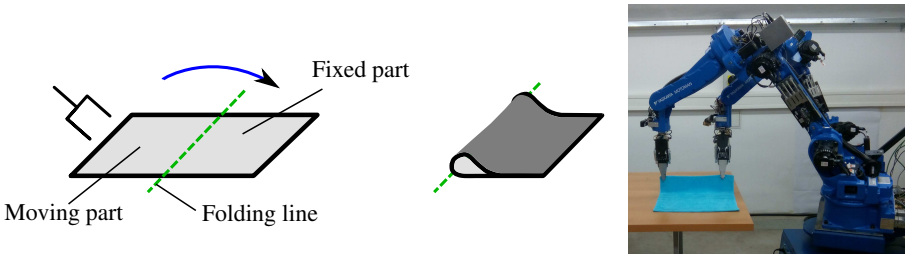

Fig. 1. The accurate folding visualization for the simplest scenario, where folding line (green, dashed) divides the sheet into two equally sized parts. The one side of the sheet is grasped and folding trajectory is followed in order to move the moving part on the top of the fixed part. One or two grippers are required for grasping depending on the width of the sheet.

linear trajectory was compared to the circular trajectory. The circular trajectory proved to be more accurate when the folding was performed on jeans. The derivation of the circular trajectory was build on the assumption of the rigid material with frictionless joint located in the folding line. The linear as well as circular trajectory do not depend on the material properties. The design of these trajectories is thus fast and it is the preferable solution if the folding accuracy requirement is not high.

The other two approaches relay on the simulation and requires the material properties to be known in advance. The first method was designed in [5], where the simulation software Maya was used. Authors described the material by a single parameter called shear resistance. In the simulated environment, the garment with a known material is folded and the resulting shape is analyzed. The folding trajectory is parametrized by a Bézier curve and the curve parameters were optimized until a sufficiently accurate fold was obtained. The shear resistance was measured by an operator before the actual folding.

In our previous work [7], we have designed another method for folding trajectory design. Our model describes the garment by a set of ordinary differential equations derived based on the static equilibrium of forces. The linear relation between the bending moment and the garment curvature is assumed, ignoring the effect of hysteresis [4]. Single parameter is required to characterize the material properties and this material parameter is a weight to stiffness ratio. The several methods for an estimation of this parameter were described in [8] and we use technique called a free fold test, originally described in [9]. The folding trajectory is found by solving a Boundary Value Problem [1,3], where boundaries characterize the folding requirements. Our method design a single trajectory for a given material and this trajectory results in the zero displacement from the expected position. In this work, an effect of the weight to stiffness ratio estimation inaccuracy is analyzed with respect to this approach for a folding trajectory design.

The methods presented here are not restricted for analysing of the garment folding only. Our model describes a wide range of materials and the accuracy analysis can be used in other fields as well. For example, the similar model was used for the task of

undersea pipes laying using the J-lay method [10] or for a pipeline installation and recovery in deepwater [11].

3 Model

The model described in [7] will be briefly introduced in this section. The model is valid for homogeneous rectangular sheets and for homogeneous 1D strings. We have shown [7], that the material can be described by a single parameter called weight to stiffness ratio and denoted by a symbol η. The weight to stiffness ratio η is a combination of the material density ρ and the material bending stiffness K in a form:

$$\eta = \frac{\rho_a \, b \, g}{K}, \tag{1}$$

where ρ_A is area density, b is a width of a rectangle and g stands for a gravitational acceleration. In a case of a 1D string, the term $\rho_A \, b$ is replaced by a length density. The density as well as the bending stiffness are constant due to the assumed homogeneity of the material. The larger weight to stiffness ratio represents softer and/or heavier material.

According to [7], the string element (see Fig. 2) is modeled by a set of following differential equations:

$$\frac{\mathrm{d}}{\mathrm{d}s}\left(\tilde{T}(s)\cos\theta(s) + \frac{1}{\eta}\frac{\mathrm{d}^2\theta(s)}{\mathrm{d}s^2}\sin\theta(s)\right) = 0\,, \tag{2}$$

$$\frac{\mathrm{d}}{\mathrm{d}s}\left(\tilde{T}(s)\sin\theta(s) - \frac{1}{\eta}\frac{\mathrm{d}^2\theta(s)}{\mathrm{d}s^2}\cos\theta(s)\right) = 1 - f(y(s))\,, \tag{3}$$

$$\frac{\mathrm{d}x(s)}{\mathrm{d}s} = \cos\theta(s)\,, \tag{4}$$

$$\frac{\mathrm{d}y(s)}{\mathrm{d}s} = \sin\theta(s)\,, \tag{5}$$

where $\mathrm{d}s$ is an element of a string, $\theta(s)$ is an angle between the element and the horizontal axis, $\tilde{T}(s)$ is a scaled tension force $T(s)$ and $f(y(s))$ is a force used to incorporate the contact of the element s with the folding surface. The variables $x(s)$ and $y(s)$ stand for the position of the element. The scaled tension force acts in a direction, which is tangent to the element and is related to the tension force as:

$$\tilde{T}(s) = \frac{T(s)}{\rho_A \, b \, g}\,. \tag{6}$$

The contact force $f(y(s))$, which supports the part of the string laying on the table is modeled as:

$$f(y(s)) = \frac{1}{y^2}10^{-6}\,, \tag{7}$$

which implies that the folding surface is horizontal with the zero height. The force is already normalized by the term $\rho_A \, b \, g$.

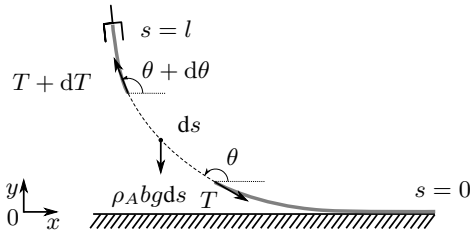

Fig. 2. The model of the string.

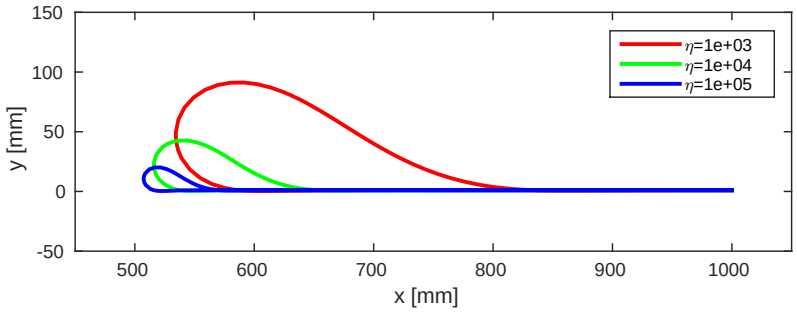

Fig. 3. Folded states for different weight to stiffness ratio η.

3.1 State of the Model

The model differential equations (2, 3, 4, 5) could be transformed to the six first order ordinary differential equations. Six boundary conditions (BCs) are thus required to specify the state of the model. For the string of the length l, the boundary conditions restrict the start ($s = 0$) or the end ($s = l$) of the string to be e.g. on the specific position or to have zero tension force. The BC at the position $s = 0$ are denoted by superscript '$^-$' and the BC at $s = l$ are denoted by superscript '$^+$'. When six BCs are specified, the BVP solver [3] is used to find the state of the model.

During the manipulation, there are many states of the model, which have to be solved. One such state is a completely folded string. It can be found by specifying the following boundary conditions:

$$\theta^- = 180^\circ\,, \quad \frac{\mathrm{d}\theta^-}{\mathrm{d}s} = 0\,, \quad x^- = l\,, \quad \frac{\mathrm{d}\theta^+}{\mathrm{d}s} = 0\,, \quad x^+ = l\,, \quad y^+ = 0\,. \tag{8}$$

The folded states will differ depending on the weight to stiffness ratio η. The several folded states for different weight to stiffness ratio are shown in Fig. 3. It can be seen, that the string curvature located in the folding line is changing according to η. In our experiments, we have measured the maximal height of the string in the folded state, and denoted it as h_m. This height was used to estimate η for the given material [8]. The relation between η and h_m, which was used for the estimation, is shown in Fig. 4.

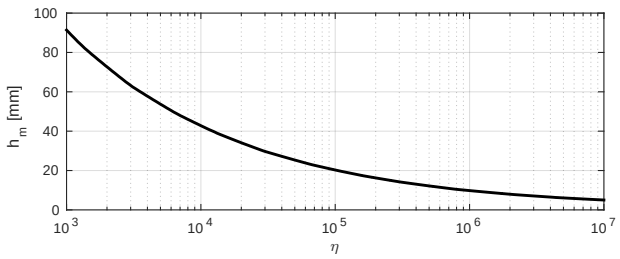

Fig. 4. Relation between weight to stiffness ratio η and maximal height of the folded string.

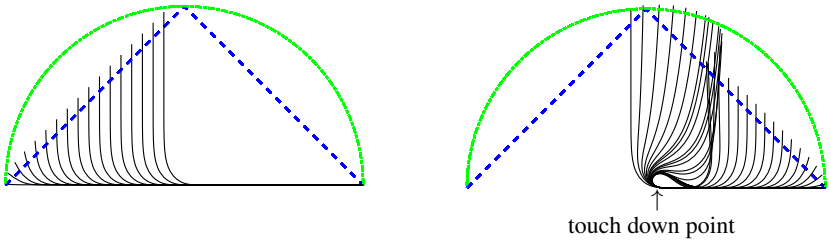

Fig. 5. Folding phases. The linear and circular trajectories are shown in blue and green, respectively. The forward folding phase is shown on the left side and backward phase is shown on the right side.

3.2 Folding Trajectory

The folding trajectory describes the pose of the robot gripper in time. In our model, the garment states satisfying the folding requirements are found and the trajectory is computed from these states. Two different types of boundary conditions were used and are denoted as the forward and the backward folding phase. Both folding phases are shown in Fig. 5. In the forward folding phase, the string is lifting until the touchdown point reaches its final position. The backward folding has a fixed touchdown point position and can be divided into two parts: (a) before the string touch itself and (b) after the touch occurs, which continues until the string is completely folded. Different weight to stiffness ratio results in different folding trajectory as shown in Fig. 6.

4 Experiments

In the ideal folding scenario, the weight to stiffness ratio η, is estimated accurately in advance. This estimate is then used to generate the folding trajectory which is executed

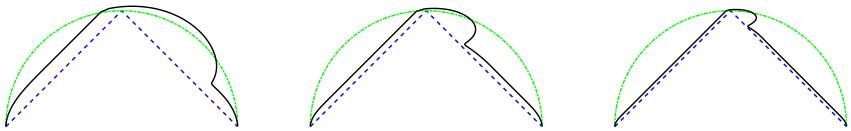

(a) $\eta = 10^3$ **(b)** $\eta = 10^4$ **(c)** $\eta = 10^5$

Fig. 6. Folding trajectory for the different weight to stiffness ratio η.

by the robot. In reality, the estimation of the weight to stiffness ratio might be inaccurate and then the designed folding trajectory is not suitable for the given material. The purpose of these experiments is to analyse the quality of the fold when η_t, used for trajectory generation, differs from the material weight to stiffness ratio η_m. We fold several materials both in simulation and in real robotic testbed and the resulting folds were analysed based on the displacement d (Fig. 7). Displacement measures the oriented distance between the expected and real position of the grasped side of the string.

Two undesirable events influence the displacement: the slipping of the strip and the bending behaviour. In this paper, the effect of bending behaviour is studied and the slipping is avoided by considering several assumptions. It is assumed, that the friction between the garment and the folding surface is high enough so the slippage of the non grasped side is zero. Furthermore, it is assumed that the friction between the garment layers is high enough as well, so the upper layer cannot slip on the lower layer. The slipping of the upper layer is unfavorable because it is hard to predict the amount of the slippage due to the elasticity of the real material and due to the high variance of the soft material friction behavior. Furthermore, it is not decidable in our model whether the upper layer will slip on the lower layer or the both layers will slip on the folding surface.

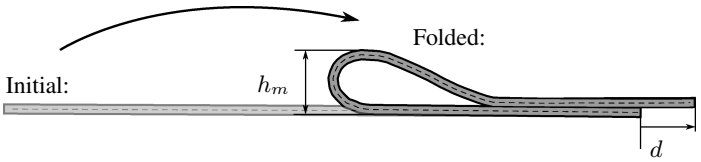

Fig. 7. The displacement measurement. The displacement d measures the quality of the fold and the maximal height h_m is used to estimate the material weight to stiffness ratio η_m.

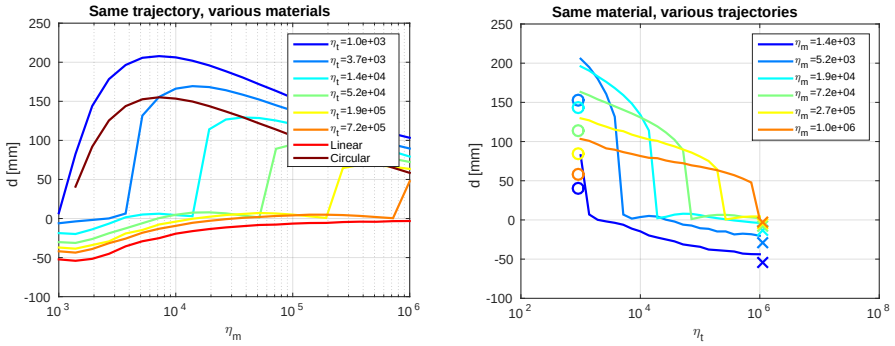

Fig. 8. Simulated displacements - two different visualizations of the same experiment. The displacements for the selected trajectories (generated with η_t) are shown for all simulated materials η_m on the left side. On the right side, the displacements of the selected materials are shown for all trajectories. The cross and circle marker stand for the linear and circular trajectory, respectively.

4.1 Simulated Displacement

To obtain the simulated displacement, the boundary conditions have to be modified such that the given trajectory $\boldsymbol{u}(t) = \left[u_x(t)\,,\, u_y(t)\,,\, u_\theta(t)\right]^\top$ can be followed. The slippage of the upper layer is forbidden in the simulation and the after touch correction of the displacement is not possible. The simulation is described by the following BCs:

$$\theta^- = 180^\circ\,, \quad \frac{\mathrm{d}\theta^-}{\mathrm{d}s} = 0\,, \quad x^- = l\,,\ \theta^+ = u_\theta\,, \quad x^+ = u_x\,, \quad y^+ = u_y\,. \tag{9}$$

The simulation is stopped when the upper layer touches the lower layer and the displacement is computed.

For the purpose of the experiments, 24 different trajectories were generated. Two of these trajectories were linear [2] and circular [6]. Other trajectories were generated for η_t interpolated logarithmically between the values: 10^3 and 10^6. These trajectories were then used to fold several materials, which differ in weight to stiffness ratio η_m in a range from 10^3 to 10^6. The measured displacements are shown in Fig. 8. It can be seen, that the displacement is zero in the case where $\eta_t = \eta_m$. It represents the situation in which the weight to stiffness ratio was estimated accurately before trajectory generation - i.e. the ideal scenario. The displacement is more or less enlarging as the estimation is moving away from the ideal scenario. Furthermore, the displacement is not symmetric. For the situation where $\eta_t > \eta_m$, the displacement is lower then for the situations where $\eta_t < \eta_m$. It suggests that one should select the trajectory on the pliable end of the known range of the material weight to stiffness ratio η. It means, that for the given η_m, we should use the larger η_t for the trajectory generation. It will results in the satisfactory folding for all materials in the range. Moreover, the smaller range will results in smaller displacement.

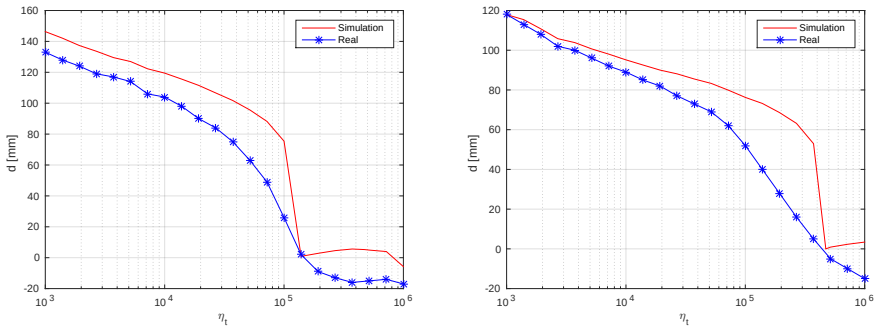

(a) $\eta_m = 1.4 \cdot 10^5$ **(b)** $\eta_m = 4.7 \cdot 10^5$

Fig. 9. Measured real displacement.

4.2 Real Displacement

We performed a real experiment with the CloPeMa testbed, where an industrial arm was used to fold the fabric strips. Strips with different weight to stiffness ratios were folded by each generated trajectory. The weight to stiffness ratios were estimated using the maximal height of the folded strips. To avoid the slipping of the strips on the table, the non grasped side was fixed to the table with the tape. The measured displacement together with simulated displacements for the estimated material are shown in Fig. 9. The measurements show, that simulation overestimated the oriented displacement for all situations except one, where $\eta_t = \eta_m$. Nevertheless, the hypothesis that trajectory on the pliable end should be selected is confirmed for the real displacements too.

4.3 Model Inconsistency

The simulated displacements overestimation suggests that there is an inconsistency in our model. To analyse this inconsistency, we performed two experiments: the first to check the repeatability of the real displacement and the second to compare simulated and real shapes of the strips during folding.

The repeatability experiment was performed for one trajectory ($\eta_t = 3.7 \cdot 10^5$) and one strip ($\eta_m = 5.5 \cdot 10^4$). The strip was folded 5 times and the measured variance of the displacement was 0.5 mm. It shows satisfactory repeatability of the real robotics folding.

The second experiment compares the simulated and real strip states. For the comparison purposes, the camera was added to the testbed and its field of view was geometrically calibrated. The calibration was used to project the simulated model into the image. The simulated state and the real state were compared visually. We observed, that the model is inconsistent in the states shown in Fig. 10. The inconsistency is probably caused by the missing hysteresis model between the bending moment and the curvature. The hysteresis modeling in the bending of fabrics was described in work [4]. In our future work, we will add the hysteresis component into our simulation in order to resolve

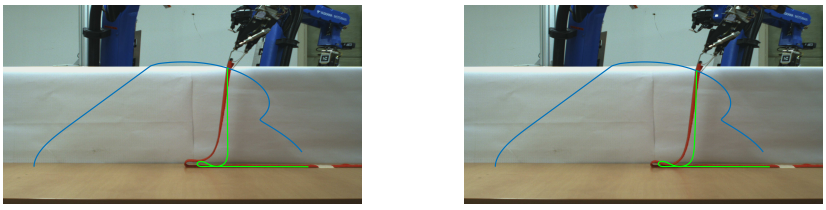

(a) Inconsistency start **(b)** Inconsistency touch real

Fig. 10. The inconsistency in the model bending behaviour. The real strip is red, the simulated is shown in green color and the followed trajectory is blue. The difference between the simulation and the real strip was negligeble until the situation shown in 10a was reached. During the situation 10a, the simulatated model skips in a single step considerably. The real strip catches up the simulation with a small delay but the touch point was shifted w.r.t. shown in simulation 10b.

this inconsistency. The bending model will then be nonlinear and the more complex estimation technique for material properties will need to be developed. Nevertheless, this inconsistency in the model does not influence the selection of the folding trajectory for the fabrics.

4.4 Fabric Folding

Our last experiment measured the displacement for whole range of typical fabrics when folded by four trajectories only. We divided the fabrics strips into four categories based on the estimated weight to stiffness ratios η_m. For these categories, the trajectory on the pliable end of the range (generated by η_t) is selected and the folding is performed on the CloPeMa testbed. The measured displacements are shown in Tab. 1. The table shows, that displacement is maximally 10 mm for all used fabric strips of length 1000 mm. For the purpose of robotic garment folding, this is an acceptable displacement. The displacement can be further reduced if more categories are used.

5 Conclusions

This contribution examined the robotic folding accuracy as a function of the material weight to stiffness ratio η. Several experiments were conducted in simulation as well as in real robotic testbed. The experiments measured the folding accuracy based on the displacement of the excepted and the real position of the grasped side of the completely folded strip. Different materials, varying in weight to stiffness ratio η were folded and we observed that the trajectory on the pliable end of the known range provides the satisfactory folding accuracy. Based on the observation, we proposed a methodology for folding of the materials with roughly estimated weight to stiffness ratio. The methodology designs a trajectory for the range of the weight to stiffness ratio and accurate

material	h_m [mm]	η_m	η_t	d [mm]
georgette	12	$4.7 \cdot 10^5$	$5.2 \cdot 10^5$	-5
chiffon	14	$3.2 \cdot 10^5$	$5.2 \cdot 10^5$	-9
acetate lining	16	$2.1 \cdot 10^5$	$5.2 \cdot 10^5$	-10
twill	17	$1.7 \cdot 10^5$	$1.9 \cdot 10^5$	-8
wool suiting	18	$1.6 \cdot 10^5$	$1.9 \cdot 10^5$	-6
herringbone pattern	19	$1.3 \cdot 10^5$	$1.9 \cdot 10^5$	-7
coating	20	$1.0 \cdot 10^5$	$1.9 \cdot 10^5$	-9
terry cloth	21	$9.0 \cdot 10^4$	$1.0 \cdot 10^5$	-7
denim	22	$7.7 \cdot 10^4$	$1.0 \cdot 10^5$	-4
plain weave	22	$7.7 \cdot 10^4$	$1.0 \cdot 10^5$	-6
chanel	25	$5.2 \cdot 10^4$	$7.2 \cdot 10^4$	-3

Table 1. Measured displacements when only four trajectories are used for fabric strips folding. The estimated weight to stiffness ratio is denoted η_m and the weight to stiffness ratio η_t was used to generate the folding trajectory. The height of folded strip h_m was used for the estimation.

estimation is thus not necessary. The demonstration of the methodology was provided for the fabric strips. We shown, that only four trajectories are required to fold all typical fabrics used for the garments.

In the experiments, we observed the inconsistency between the simulation and real strips. This inconsistency causes an overestimation of the simulated displacement. We think, the inconsistency can be resolved by adding the hysteresis into the model and we will address this task in the future work.

Acknowledgment

This work was supported by the Technology Agency of the Czech Republic under Project TE 01020197 Center Applied Cybernetics, the Grant Agency of the Czech Technical University in Prague, grant No. SGS15/203/OHK3/3T/13.

References

1. Bellman, R.E., Kalaba, R.E.: Quasilinearization and nonlinear boundary-value problems. Tech. rep., RAND Corporation, Santa Monica (1965) 3
2. van den Berg, J., Miller, S., Goldberg, K.Y., Abbeel, P.: Gravity-based robotic cloth folding. In: Int. Workshop on the Algorithmic Foundations of Robotics (WAFR). pp. 409–424 (2010) 2, 8
3. Kierzenka, J.A., Shampine, L.F.: A bvp solver that controls residual and error. J. Numer. Anal. Ind. Appl. Math (JNAIAM) pp. 1–2 (2008) 3, 5
4. Lahey, T.: Modelling hysteresis in the bending of fabrics (2002) 3, 9
5. Li, Y., Yue, Y., Xu, D., Grinspun, E., Allen, P.K.: Folding deformable objects using predictive simulation and trajectory optimization. In: Proc. Int. Conf. on Intelligent Robots and Systems (IROS). IEEE/RSJ (2015) 3

6. Petrík, V., Smutný, V., Krsek, P., Hlaváč, V.: Robotic Garment Folding: Precision Improvement and Workspace Enlargement. In: Annu. Conf. Towards Autonomous Robotic Systems (TAROS). pp. 204–215 (2015) 2, 8
7. Petrík, V., Smutný, V., Krsek, P., Hlaváč, V.: Physics-based model of rectangular garment for robotic folding. Research Report CTU–CMP–2016–06, Center for Machine Perception, K13133 FEE Czech Technical University, Prague, Czech Republic (May 2016) 3, 4
8. Plaut, R.H.: Formulas to determine fabric bending rigidity from simple tests. Textile Research Journal 85(8), 884–894 (2015) 3, 5
9. Stuart, I.: A loop test for bending length and rigidity. British Journal of Applied Physics 17(9), 1215 (1966) 3
10. Wang, L.z., Yuan, F., Guo, Z., Li, L.l.: Numerical analysis of pipeline in j-lay problem. Journal of Zhejiang University SCIENCE A 11(11), 908–920 (2010) 4
11. Zeng, X.G., Duan, M.L., An, C.: Mathematical model of pipeline abandonment and recovery in deepwater. Journal of Applied Mathematics 2014 (2014) 4